RESEARCH ARTICLE

Phycological
Society of America

The challenge of estimating kelp production in a turbid marine environment

Kiara Franke[1,2] | **Lisa C. Matthes**[2,3,4] | **Angelika Graiff**[2] | **Ulf Karsten**[2] | **Inka Bartsch**[4]

[1]Alfred-Wegener-Institut, Helmholtz-Zentrum für Polar- und Meeresforschung (AWI), 27570, Bremerhaven, Germany

[2]Institute of Biological Sciences, Applied Ecology and Phycology, University of Rostock, 18059, Rostock, Germany

[3]Takuvik International Research Laboratory, Université Laval and CNRS, G1V0A6, Québec, Canada

[4]Alfred Wegener Institute, Helmholtz-Centre for Polar and Marine Research, 27570, Bremerhaven, Germany

Correspondence
Kiara Franke, Institute of Biological Sciences, Applied Ecology and Phycology, University of Rostock, 18059 Rostock, Germany.
Email: kiara.franke@uni-rostock.de

Abstract

Coastal kelp forests produce substantial marine carbon due to high annual net primary production (NPP) rates, but upscaling of NPP estimates over time and space remains difficult. We investigated the impact of variable underwater photosynthetically active radiation (PAR) and photosynthetic parameters on photosynthetic oxygen production of *Laminaria hyperborea*, the dominant NE-Atlantic kelp species, throughout summer 2014. Collection depth of kelp had no effect on chlorophyll *a* content, pointing to a high photoacclimation potential of *L. hyperborea* towards incident light. However, chlorophyll *a* and photosynthesis versus irradiance parameters differed significantly along the blade gradient when normalized to fresh mass, potentially introducing large uncertainties in NPP upscaling to whole thalli. Therefore, we recommend a normalization to kelp tissue area, which is stable over the blade gradient. Continuous PAR measurements revealed a highly variable underwater light climate at our study site (Helgoland, North Sea) in summer 2014, reflected by PAR attenuation coefficients (K_d) between 0.28 and 0.87 m^{-1}. Our data highlight the importance of continuous underwater light measurements or representative average values using a weighted K_d to account for large PAR variability in NPP calculations. Strong winds in August increased turbidity, resulting in a negative carbon balance at depths >3–4 m over several weeks, considerably impacting kelp productivity. Estimated daily summer NPP over all four depths was 1.48 ± 0.97 g C $\cdot$ m^{-2} seafloor $\cdot$ d^{-1} for the Helgolandic kelp forest, which is in the range of other kelp forests along European coastlines.

KEYWORDS
diffuse vertical attenuation coefficient, dry mass:area-ratio, Helgoland, kelp, oxygen evolution, photoacclimation, primary production

INTRODUCTION

Brown algae of the order Laminariales make up the majority of macroalgal biomass in the world's temperate and high-latitude shallow rocky coastal areas of the Northern hemisphere (Steneck et al., 2002), reaching annual net primary production (NPP) rates between 166 and 1780 g C $\cdot$ m^{-2} seafloor $\cdot$ y^{-1} (Duarte et al., 2022; Mann, 2000; Pedersen et al., 2020; Smale et al., 2020). Due to their high production rates, these macroalgal communities represent important links in the marine nutrient and carbon cycle. One of these links is

---

Abbreviations: ^{14}C, radio-labeled carbon; DA, disc area; DM, dry mass; FM, fresh mass; K_d, diffuse vertical attenuation coefficient; LAI, leaf area index; MLWS, mean low water spring tide; NPP, net primary production; PI, photosynthesis versus irradiance; PQ, photosynthetic quotient.

the large export of seaweed detritus to adjacent areas where it fuels secondary production or becomes buried in marine sediments as blue carbon (Krause-Jensen & Duarte, 2016; Pedersen et al., 2020). Therefore, reliable macroalgal primary production estimates obtained over the annual cycle and along environmental gradients are crucial for assessing the role of kelp forests in the local and global carbon cycles.

Kelp species can be observed in the rocky sublittoral zone around the world (e.g., Krause-Jensen et al., 2012, 2020; Pehlke & Bartsch, 2008; Smale et al., 2020) and are thereby exposed to regular changes in water levels throughout the tidal cycle and to intense wave motion during storm events. The resulting sediment re-suspension in combination with terrestrial input of dissolved and particulate organic matter can reduce underwater light availability significantly in the coastal environment (Lüning & Dring, 1979). Light is one of the main factors physiologically constraining the global distribution of kelp forests next to substrate availability, water temperature, and nutrients (Assis et al., 2016; Bolton & Lüning, 1982; Steneck et al., 2002). Kelp species have to acclimatize to considerable daily and seasonal (sun angle, day length, cloud cover, and tidal cycles) variations in incident irradiance along their depth distribution to reach high production rates and efficiently convert carbon dioxide into carbohydrates such as the storage compounds mannitol and laminarin, which are used to support growth in low-light periods during winter (Lüning, 1979, 1990).

Kelp primary production can be estimated from standing crop (expressed in fresh mass, dry mass, or blade area), population density, and growth rate or by measuring gas exchange in terms of either the oxygen released or the radio-labeled carbon (^{14}C) assimilated (Iñiguez et al., 2016; Lüning, 1969; Pedersen et al., 2012; Smale et al., 2020). Oxygen production and uptake in an entire individual or excised blade tissue are measured either ex situ in the laboratory or in situ in submerged chambers, and both measures have been widely used to study the physiology and biomass production of macroalgae (e.g., Colombo-Pallotta et al., 2006; Liu et al., 2018; Staehr & Wernberg, 2009; White et al., 2021). In order to derive the amount of fixed carbon as the ultimate and widely comparable measure of production, oxygen-release values have to be converted into units of fixed carbon using the photosynthetic quotient (PQ). The PQ is defined as the molar ratio of oxygen (gross oxygen evolution) produced to carbon dioxide (gross carbon fixation) assimilated during photosynthesis (Iñiguez et al., 2016); however, PQ values are variable, species-specific, and often unknown (Buesa, 1980; Iñiguez et al., 2016; Miller III et al., 2009). In addition, acquiring primary production measurements of kelp species remains challenging due to the high level of thallus differentiation and the resulting variability in structure and metabolically active tissue (Gómez et al., 2016; Küppers & Kremer, 1978; Steinbiss

& Schmitz, 1974). These studies have shown that photosynthetic activity varies along the thallus gradient and that production estimates from one region of the blade should be handled with care when normalized to different parameters (e.g., fresh mass versus dry mass). Additionally, the photosynthetic performance of individuals can vary with depth and decreasing light levels as Koch et al. (2016) have shown for *Macrocystis pyrifera*.

Laminaria hyperborea is the biomass-dominant kelp species in the rocky mid-sublittoral along the European coastline (Assis et al., 2016; Smale et al., 2020). Its distribution range stretches from northern Portugal (Araujo et al., 2009) to northern Norway (Kylin, 1947; Lüning, 1990). In the southern North Sea, the rocky island of Helgoland (Germany) represents a hotspot of marine biodiversity and is surrounded by a unique kelp forest (Lüning, 1969), with *L. hyperborea* representing the biomass-dominant kelp species between 1 and 12.5 m depths (Pehlke & Bartsch, 2008). While quantitative data about biomass distribution and blade area of this species are available (Lüning, 1969; Pehlke & Bartsch, 2008; Steinberg, 2019), NPP estimates are still lacking.

To address this lack of knowledge, the present study provides first estimates of *Laminaria hyperborea* NPP at the island of Helgoland, measured during summer 2014 when annual incident solar radiation and water temperature were highest. Oxygen optode incubation methods were used to derive photosynthetic parameters of adult *L. hyperborea* sporophytes from fitted photosynthesis versus irradiance (PI) curves. Retrieved photosynthetic rates were correlated with continuous in situ underwater PAR measurements at different depth levels derived from K_d values and later converted into carbon fixation (C-fixation) rates. These rates were multiplied with *L. hyperborea* blade area per square meter seafloor to calculate mean daily summer NPP integrated over depth. Here, we show how large variations observed in incident underwater irradiance caused by changing surface conditions, ranging from calm and sunny to windy and cloudy, affect seasonal NPP calculations with different PAR inputs. The dataset was also used to develop a framework of how to generate more reliable NPP rates based on ex situ photosynthetic measurements.

Specifically, our objectives were (1) to assess the influence of variations in photosynthetic performance and chlorophyll *a* (Chl *a*) concentration of *Laminaria hyperborea* along its depth distribution and along its blade gradient when normalized to two different parameters used in photosynthesis measurements (fresh mass and blade area), (2) to investigate the variability of the underwater light climate in the sublittoral throughout summer and its impact on seasonal NPP estimations along the depth gradient, and finally, (3) to calculate the first estimate of daily summer NPP of *L. hyperborea* off Helgoland per unit seafloor.

METHODS

Study site, sampling, and material

Adult *Laminaria hyperborea* (hereafter called *L. hyperborea*) sporophytes were collected from the sublittoral zone along a depth gradient at 0.5, 2, 4, 6±0.2 m mean low water spring (MLWS; depth measured at the holdfast) off the island of Helgoland (North Sea, Germany; 54°11'17" N°52'12" E) between 17 July and 12 September 2014 (Figure 1). The sampling locations followed a depth transect through the main *L. hyperborea* forest north of the island (Uhl et al., 2016) stretching approximately 1.4 km (Figure 1). Sampling at each target depth took place over a period of 7 weeks for 9 d in total. Due to intermediate rough weather conditions, the sampling period had to be extended. Very warm weather also resulted in degradation of the material in one case, so that sampling had to be repeated (Table 1). At 0.5 m target depth, samples were taken and processed only once. At 2 and 4 m target depths, three dives per depth were conducted, and after each dive, two individuals out of nine were selected for incubations that same day to keep the material as fresh as possible. At 6 m target depth, two sampling and incubation days were needed for completion of all replicate measurements (Table 1).

Seawater temperature and salinity were 18±2°C and 31±1 S_A (absolute salinity), respectively, at 10 m (MLWS) during the sampling period (CTD2 Underwater Node Helgoland, COSYNA data web portal: http://codm.hzg.de/codm/).

At each depth, three 1 m² quadrats were placed by SCUBA divers, and within these, three individuals with the longest stipe and with the blade (visually) least covered by epibionts were removed completely, resulting in a total of nine individuals per sampling depth (Figures 2a,b). Due to the uneven underwater topography of the northern sublittoral zone, quadrats were placed as haphazardly as possible in the sampling area at the target depth during each dive. As the topography off Helgoland is rough with canyons and ridges alternating along short distances, kelp individuals are not evenly spread along the seafloor but grow quite patchy, especially at depths ≥4 m. Thus, usage of random numbers was not applicable for our purpose. All *Laminaria hyperborea* samples were carried to the laboratory in dark plastic bags with constant natural seawater flow. Directly after sampling, kelp individuals were transferred into two 60 L basins, freshly filled with cooled (approximately 15°C) pre-filtered seawater and stored in the dark in the culture room. For the following photosynthesis incubation experiments, the individuals with the lowest visible coverage of epi- and endobionts from each depth were chosen. Measurements always took place the day after sampling. For details, see Table 1. One hour after the transfer of the sampled kelp individuals into the laboratory, blade tissue was excised for the two experiments:
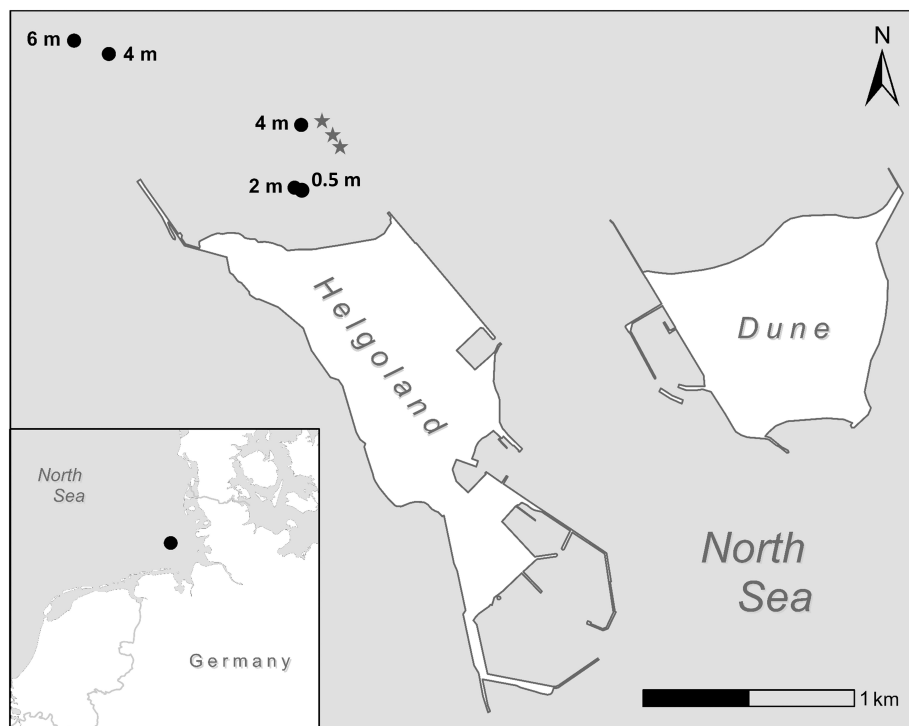
FIGURE 1 Study site in the north-western rocky sublittoral off Helgoland, Germany. Locations of the *Laminaria hyperborea* sampling stations at different depths (mean low water spring tide) are shown as black circles and locations of underwater light loggers are shown as gray stars.

Experiment 1 - Depth gradient: Three neighboring blade discs per individual were cut with a cork borer (Ø 1.7 cm) at 25 cm (medial) distance above the stipe-blade transition zone.

Experiment 2 - Blade gradient: From the material collected at 2 and 4 m depths, three additional blade discs (Ø 1.7 cm) were cut per individual at 5 cm (basal) and 50 cm (distal) distance above the stipe-blade transition zone (Figure 2d).
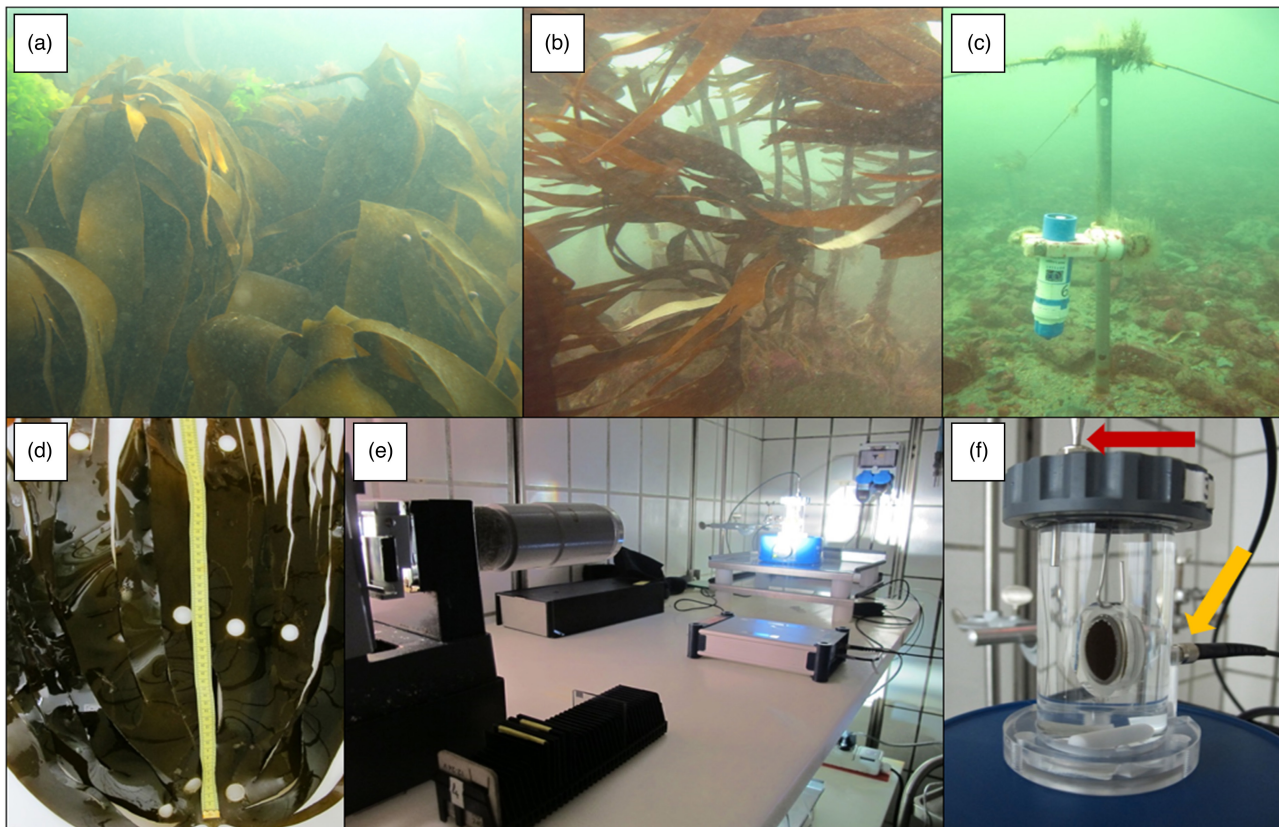
After excision, the three discs per individual for the depth gradient (nine discs per individual for the blade gradient) were cultivated separately in filtered

TABLE 1 Sampling days of *Laminaria hyperborea* individuals for the two experiments at each target depth during summer 2014.

Depth (m)	Sampling date in 2014		
0.5	8 Aug (6/6)		
2	22 Aug (2/6)	27 Aug (2/6)	6 Sep (2/6)
4	24 Jul (2/6)	1 Aug (2/6)	15 Aug (2/6)
6	4 Aug (4/6)		3 Sep (2/6)

Note: The number of individuals measured during the respective next 2 days is given in brackets. The second number shows the respective number of replicates.

seawater in 1-L Nalgene flasks in a temperature-controlled room at $13.5 \pm 0.5°C$ in the dark, over-night. This procedure aimed to reduce increased respiration rates associated with cutting (Bidwell & McLachlan, 1985; Hatcher, 1977), to reduce mucus excretion, and to enable the formation of new medullary cells and epidermis along the cut edges (Lüder & Clayton, 2004). Directly after cutting and on the following morning, the potential maximum quantum yield of PSII (F_v/F_m) of each of the three discs per individual for the depth gradient (nine discs per individual for the blade gradient) was measured. The disc with the best F_v/F_m value per individual and distance was chosen for oxygen incubation, resulting in $n = 6$ for each PI measurement for both experiments. Due to logistical constraints of only performing three measurements in parallel, three discs were measured in the morning and in the afternoon, thereby also accounting for the diurnal variance known to be inherent in seaweed photosynthetic activity (Granbom et al., 2001; Henley et al., 1991; Schubert et al., 2004). For a better understanding, the complex sampling design and workflow is visualized in Figure S1 in the Supporting Information.

FIGURE 2 Sampling procedure and set-up for photosynthesis versus irradiance measurements. *Laminaria hyperborea* forest at (a) 0.5 m and (b) 6 m depth (mean low water spring tide). (c) Photosynthetically active radiation logger at 6 m. (d) Blade of *L. hyperborea* with cut-out discs at three regions (basal, medial, and distal) above the stipe-blade transition zone. (e) Oxygen production measurement set-up in temperature-constant room showing slide projector and (f) incubation chamber with the mounted kelp disc, temperature sensor (upper arrow) and optical fiber attachment (lower arrow). [Color figure can be viewed at wileyonlinelibrary.com]

TABLE 2 Details of the photosynthesis versus irradiance experiments.

Experiment	Depth (m)	Replicates per depth	Blade region	PFD levels (μmol photons $\cdot$ m$^{-2} \cdot$ s^{-1})	Exposure time per light step (min)	Dark incubation (min)
Blade gradient	2, 4	6	Basal, medial, distal	3–560	10	20
Depth gradient	0.5, 2, 4, 6	6	Medial			

Note: Basal: 5 cm, medial: 25 cm, distal: 50 cm from the stipe-blade transition zone. PFD: Photon flux density

Maximum quantum yield

The in vivo Chl *a* fluorescence of photosystem II (PSII) of freshly cut and dark-acclimated (12 h) discs was measured using pulse-amplitude-modulated fluorometry (PAM 2100, WALZ, Germany) as described by Schreiber et al. (1986). These measurements were performed before the oxygen incubations to verify that discs were in good physiological condition. Minimum (F_0) and maximum fluorescence (F_m) of samples were measured, and F_v/F_m was calculated.

Photosynthesis versus irradiance measurements

Net oxygen flux of incubated *Laminaria hyperborea* discs was measured using an oxygen optode system and applying PI relationships to investigate the photosynthetic performance along the depth (experiment 1) and blade gradient (experiment 2). Measurements were performed the day after disc cutting in a temperature-constant room at 12 ± 0.5°C. Photosynthetic oxygen flux of each disc was measured in a constantly stirred circular 80-mL airtight acrylic glass chamber. Before each measurement, the *L. hyperborea* disc was fixed in an acrylic glass ring attached to the chamber filled with sterile filtered seawater and orientated perpendicular to the light source (Figure 2e,f). The sterile filtered seawater medium was enriched with 8 mL Tris buffer (1.0 M, pH 8.0, Merck Millipore, Germany) and 0.42 g sodium bicarbonate (NaHCO$_3$, 5.0 mM, Merck Millipore, Germany) per liter medium to prevent bicarbonate depletion (Johnston & Raven, 1986) and was initially flushed with gaseous nitrogen to an initial dissolved oxygen (O$_2$) concentration of 70%–80% of air saturation. After-closure changes in O$_2$ within the chamber were determined every 10 s by fiber-optic oxygen micro-optodes (Fibox 3, PreSens) with a Pt1000 temperature sensor and a 2-mm thick polymer optical fiber connected to a non-invasive fluorescent oxygen sensor spot (type PSt3, PreSens, Regensburg, Germany; Figure 2f). Oxygen sensor spots were only used after two-point calibration with oxygen-free and oxygen-saturated seawater, which was repeated every 3 weeks. Oxygen-free water was achieved by dissolving 1 g of sodium sulfite (Na$_2$SO$_3$, M = 126 g/L, Carl Roth GmbH + Co KG, Karlsruhe, Germany) in 100 mL water. Oxygen saturation was determined in vapor-saturated

air. Incident light was generated by a slide projector (Liesegang Dianfant, Leitz Prado, Germany) equipped with a halogen lamp (Osram Xenophot 400 W/36 V, Germany) and 11 Schott neutral gray filters to achieve increasing photon flux densities (PFD) between 3 and 560 μmol photons $\cdot$ m$^{-2} \cdot$ s^{-1} (Table S1 in the Supporting Information). Irradiances were recorded with a cosine-corrected planar sensor for photosynthetically active radiation (PAR, 400–700 nm; LI-190SA quantum sensor, LI-COR Inc., USA) connected to a data logger (LI-1400 logger, LI-COR Inc).

Dark respiration of the discs was measured for 20 min before and after the exposure to the increasing PFD levels; all 11 PFDs were measured in 10-min intervals (Table 2). Oxygen concentration expressed in % air saturation was logged by the OxyView software (Presens) and corrected for air pressure, salinity, and logged temperature in accordance with Tengberg et al. (2006). During post-processing, the oxygen production rate for each PFD level was calculated by plotting a linear regression model through all O$_2$ values measured during the time interval and was normalized to either fresh mass (FM, unit: μmol O$_2 \cdot$ g^{-1} FM $\cdot$ h^{-1}) or disc surface area (DA, unit: μmol O$_2 \cdot$ cm^{-2} DA $\cdot$ h^{-1}). Oxygen incubations of samples from the same depth and blade section were performed in replicates of six, always three in the morning and three in the afternoon, to account for the diurnal variability of photosynthetic activity (Hanelt et al., 1993; Figure S1). FM of each disc was determined after the oxygen measurements.

To calculate photosynthetic rates, oxygen production and respiration rates of every disc along the blade and depth gradient were plotted against irradiance. PI curves were fitted by minimizing the sum of differences between the measured oxygen flux and the model proposed by Jassby and Platt (1976):

$$P = P_{max} \times \tanh\left(\frac{\alpha \times I}{P_{max}}\right) + R \quad (1)$$

where P is oxygen production rate (μmol O$_2 \cdot$ g^{-1} FM $\cdot$ h^{-1} or μmol O$_2 \cdot$ cm^{-2} DA $\cdot$ h^{-1}), at a given irradiance I (PAR, μmol photons $\cdot$ m$^{-2} \cdot$ s^{-1}). The maximum oxygen production rate is P_{max} (μmol O$_2 \cdot$ g^{-1} FM $\cdot$ h^{-1} or μmol O$_2 \cdot$ cm^{-2} DA $\cdot$ h^{-1}); the light utilization coefficient is α (μmol O$_2 \cdot$ g^{-1} FM $\cdot$ h^{-1} (μmol photons $\cdot$ m$^{-2} \cdot$ s^{-1})$^{-1}$ or μmol O$_2 \cdot$ cm^{-2} DA $\cdot$ h^{-1} (μmol photons $\cdot$ m$^{-2} \cdot$ s^{-1})$^{-1}$); and the initial dark respiration rate is R (μmol O$_2 \cdot$ g^{-1} FM $\cdot$ h^{-1} or μmol O$_2 \cdot$ cm^{-2} DA $\cdot$ h^{-1}). The light saturation

point I_k (μmol photons $\cdot$ m^{-2} $\cdot$s^{-1}) was calculated by dividing P_{max} by α. The light compensation point I_c (μmol photons $\cdot$ m^{-2} $\cdot$ s^{-1}), at which photosynthesis equals respiration, was obtained from the intersection of the curve with the x-axis.

Chlorophyll *a* concentration

After termination of the oxygen incubations, discs were flash-frozen in liquid nitrogen and stored at –80°C for up to 7 weeks until all discs had been freeze-dried for approximately 36 h (Beta 1–8 LDplus, Christ, Osterode am Harz, Germany). Before pigment extraction, freeze-dried discs were finely ground for several minutes using steel grinding balls (3 mm diameter) in a Mikro-Dismembrator U (Braun Biontech International, Melsungen, Germany) at a frequency of 2000 shakes per minute. Chl *a* concentration of each disc was analyzed following a modified method after Inskeep and Bloom ([1985](#)). Approximately 20% of the ground disc material (0.01–0.04 g) was used to extract Chl *a* in 5 mL of N,N-dimethylformamide (DMF) in the dark at 4°C for 4 d. Afterward, the extract was centrifuged for 8 min at 252 *g* in a cooled centrifuge (Centrifuge 3 K10, Sigma, Osterode, Germany). The Chl *a* concentration of the supernatant was determined using a spectrophotometer (U-3310, Hitachi High-Tech, Japan) at two wavelengths (347 and 664.5 nm), and Chl *a* was normalized to FM (Chl a_{FM}) and DA (Chl a_{DA}) as follows:

$$\text{mg Chl } a \bullet \text{g}^{-1}\text{FM} = \left(12.7 \bullet \text{Extinction}_{664.5 \text{ nm}} \bullet \frac{\text{DMF(mL)}}{1000} \right) \bullet \text{FM}(\text{g}^{-1}) \tag{2}$$

$$\text{mg Chl } a \bullet \text{cm}^{-2}\text{DA} = \left(12.7 \bullet \text{Extinction}_{664.5 \text{ nm}} \bullet \frac{\text{DMF (mL)}}{1000} \right) \bullet \text{DA (cm}^{-2}) \tag{3}$$

Underwater irradiance measurements

Underwater irradiance was recorded with cosine-corrected planar PAR loggers (Odyssey Photosynthetic Irradiance Recording System, Dataflow Systems PTY Limited, New Zealand) at four depths: 1.2, 2.9, 4.4, and 6.6 m (MLWS; Figure 2c). Odyssey PAR loggers were calibrated against a cosine-corrected planar PAR sensor (LI-190SA quantum sensor, LI-COR Inc., USA) over a 24-h period at 4 m depth in the Helgolandic South harbor. During the sampling period between 18 June and 11 September 2014, incoming PAR was recorded continuously every 15 min at 1.2 and 2.9 m and every 30 min

at 4.4 and 6.6 m in the northern sublittoral (Figure 1). No PAR was recorded on 24 July or 1 August, nor between 25 and 28 August due to sensor removal for data download and, in late August, unsafe weather conditions that prevented a timely redeployment. To avoid biofouling of the sensor heads, PAR loggers were cleaned every week (1.2 m) or every second week (all other depths) by SCUBA divers. The diffuse vertical attenuation coefficient K_d (PAR, m^{-1}) of downward PAR (I_d, z) for each hour of each day was determined by the slope of the linear regression between the natural logarithm of measured PAR and the four depth levels (Morris et al., [1995](#)).

Calculation of daily net production

Daily NPP of *Laminaria hyperborea* was calculated by correlating the PI parameters obtained in vitro with continuous in situ PAR data at the mean depth of the *L. hyperborea*. Therefore, irradiance, I_d (z_2), available at the holdfast depths was estimated by applying Beer–Lambert's Law:

$$I_d\left(z_2, \text{PAR} \right) = I_d(0^-, \text{PAR}) \bullet e^{\left(-K_d(\text{PAR}) \bullet (z_2 - z_1) \right)} \tag{4}$$

including the calculated hourly K_d (PAR) and the downward irradiance of PAR (I_d, 0^-) just below the water surface. Beforehand, I_d (0^-) was estimated for every 15 min using Equation 4 with calculated hourly K_d (PAR) and in situ I_d (z_2) at z_2 = 1.2 m, which was measured every 15 min. The PI parameters (P_{max}, R, α; normalized to DA as this was independent from depth and blade gradient), measured in medial discs and estimated I_d (z), were used in Equation 1 to calculate net oxygen production rates (μmol O_2 $\cdot$ cm^{-2} DA $\cdot$ 15 min^{-1}) for every 15 min during the 7 weeks at the holdfast depths (0.5, 2, 4, 6 m ± 20 cm) following the concept of Deregibus et al. ([2016](#)). The calculated oxygen production rates in micromoles from all 96 measurements of 1 d were divided by 4 to correct for hourly values over the 24-h period and converted to mol O_2 $\cdot$ cm^{-2} DA $\cdot$ h^{-1}. The resulting net oxygen production rates were converted to C-fixation rates using the molar weight of carbon of 12.011 g $\cdot$ mol^{-1} and a PQ of 1.18 (Miller III et al., [2009](#)) according to:

$$\text{NPP} \left(\text{g C} \bullet \text{cm}^{-2}\text{DA} \bullet \text{h}^{-1} \right) = \frac{\text{NPP} \left(\text{mol } O_2 \bullet \text{cm}^{-2}\text{DA} \bullet \text{h}^{-1} \right)}{1.18 \text{ mol } O_2 \bullet \text{mol}^{-1} \text{ C}} * 12.011 \text{ g C} \bullet \text{mol}^{-1} \tag{5}$$

Next, hourly C-fixation rates were summed up over the 24-h period to calculate NPP per cm^2 *L. hyperborea* DA for an entire day (g C · cm^{-2} DA · d^{-1}). Lastly, daily NPP per depth and square meter seafloor (g C · m^{-2} seafloor · d^{-1}) of the *L. hyperborea* forest at 0.5, 2, 4, and 6 m was estimated by multiplying the production rate per cm^2 *L. hyperborea* DA with the mean in situ leaf area index (LAI) of *L. hyperborea* per depth published in Pehlke and Bartsch ([2008]). This resulted in mean production rates for each depth over the 7 weeks of irradiance recordings. The final mean NPP value was calculated using the mean values across all four depths. For comparative purposes, daily NPP values were also calculated using the measured maximum and minimum daily K_d and the mean K_d, which was derived from all daily K_d over the entire sampling period.

Statistical analysis

Statistical analyses were performed in IBM SPSS Statistics (version 27.0.1). Data were analyzed in two groups: blade gradient (basal, medial, and distal discs from 2 and 4 m) and depth gradient (medial discs from all four depths). Blade gradient: Significant differences in FM, F_v/F_m, PI parameters, and Chl *a* between blade regions were assessed using a repeated measures analysis of variance (RM ANOVA) for both depths separately. Beforehand, data were tested for sphericity using Mauchly's sphericity test, and the Greenhouse–Geisser correction was used if sphericity was not given. For pairwise comparison, the significance level was adjusted with the Bonferroni correction ($p = 0.05/3 = 0.017$) due to multiple comparisons. Differences in F_v/F_m values before and after overnight cultivation were assessed using an RM ANOVA for both depths separately. Depth gradient: To compare FM, F_v/F_m, PI parameters, and Chl *a* between sampling depths, one-way ANOVAs were conducted after data were tested for normal distribution and homogeneity of variances using the Kolmogorov–Smirnov test and Levene's test, respectively. Tukey HSD post-hoc tests were performed when significant differences occurred.

To compare the impact of different K_d values, daily NPP rates were calculated using measured daily K_d values and compared to daily mean NPP rates, calculated with (1) mean daily K_d input over the entire sampling period, (2) minimum daily K_d input, and (3) maximum K_d input in non-parametric Kruskal-Wallis ANOVAs as normal distribution was not given (Kolmogorov–Smirnov-Test), for all sampling days ($n = 50$) and for each depth separately. Per depth, the overall summer NPP rates ($n = 4$) calculated using different K_d values were compared in paired-sample t-tests with Bonferroni-correction ($p < 0.013$) for multiple comparison. To evaluate the daily NPP rates based on different K_d values

and daily NPP rates based on daily calculated K_d values, the coefficient of determination (R^2) was used.

RESULTS

Physiological condition of blade discs

Directly after cutting, the F_v/F_m of *Laminaria* discs was 0.74 ± 0.02. Water depth and blade region had no significant effect on F_v/F_m, while time had a significant effect on discs of both gradients. Overnight cultivation had a significantly negative effect on F_v/F_m of discs from different blade regions (2 m: $F_{1,5} = 76.7$, $p < 0.001$; 4 m: $F_{1,5} = 9.3$, $p = 0.03$, RM ANOVAs) and different depths ($F_{1,20} = 19.3$, $p < 0.001$, one-factorial ANOVA). However, overnight samples showed F_v/F_m of 0.71 ± 0.01, which was still in the known optimum range for brown algae (0.7–0.8; Hanelt, [2018]). Fresh mass of medial discs was 0.45 ± 0.05 g and not significantly different between the four depths ($F_{3,20} = 0.8$, $p = 0.5$, one-factorial ANOVA). However, FM of discs decreased significantly from the basal (0.67 ± 0.04 g) to the distal region (0.30 ± 0.02 g) in individuals of both investigated depths (2 m: $F_{2,10} = 333$, $p < 0.001$; 4 m: $F_{2,10} = 81$, $p < 0.001$, RM ANOVAs).

Photosynthetic characteristics

Experiment 1 – Depth gradient. The impact of normalization to either FM or DA on Chl *a* and photosynthetic parameters of *Laminaria* sampled at 0.5, 2, 4, and 6 m depths in the same intermediate tissue area is exhibited in Figure 3. The depth gradient did not result in significant differences in Chl *a*, P_{max}, and α and in the reference independent I_k. Respiration rates normalized to both factors and reference independent I_c showed significant but random changes along the depth gradient (Table 3).

The mean Chl *a* concentration of *Laminaria* discs from all depths was 0.01 ± 0.002 mg · cm^{-2} DA or 0.05 ± 0.01 mg · g^{-1} FM and, although slightly decreasing at 2 m, was not significantly different (Figure 3a; Table 3). Over all depths, I_k was 70.2 ± 13.4 μmol photons · m^{-2} · s^{-1} and had highest values at 4 and 6 m without a significant difference (Figure 3c; Table 3). Similarly, maximum photosynthesis P_{max} was stable over the depth gradient irrespective of the normalization parameter with mean values of either 3.3 ± 0.5 μmol O_2 · cm^{-2} DA · h^{-1} or 17.7 ± 4.6 μmol O_2 · g^{-1} FM · h^{-1} (Figure 3d; Table 3). Along the depth gradient, α was very stable with mean values of either 0.05 ± 0.02 μmol O_2 · cm^{-2} DA · h^{-1} (μmol photons · m^{-2} · s^{-1})$^{-1}$ and 0.26 ± 0.09 μmol O_2 · g^{-1} FM · h^{-1} (μmol photons · m^{-2} · s^{-1})$^{-1}$ (Table 3; Figure 3f). In contrast, the reference independent I_c significantly varied with depth, being significantly lower at
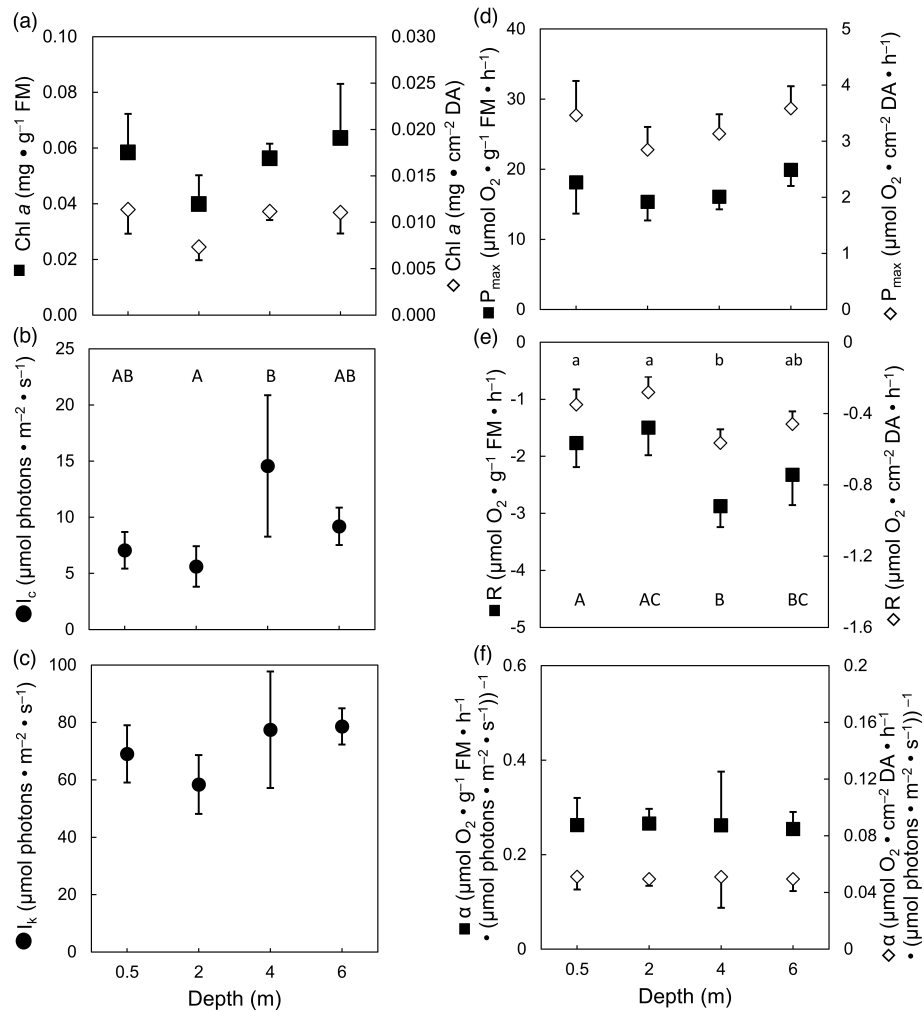
FIGURE 3 Chlorophyll *a* concentration (Chl *a*) and photosynthesis versus irradiance (PI) parameters of *Laminaria hyperborea* ($n = 6$ each depth) collected along a depth gradient (0.5–6 m). Samples were cut 25 cm above the stipe-blade transition zone. (a) Chl *a* and PI parameters, (d) P_{max}, (e) R, and (f) α, were normalized to either fresh mass (FM; black square) or disc area (DA; white diamond). Units of PI parameters, (b) I_c and (c) I_k, are independent from normalization and the same for both reference parameters (filled circles). Lower case and capital letters within each subplot show significant differences between regions related to either DA or FM, respectively (Statistical results: Table 3).

2 m than at 4 m (5.4 ± 2.9 vs. 13.2 ± 5.8 µmol photons· $m^{-2} \cdot s^{-1}$, respectively; Tukey test: $p < 0.03$), while values at 0.5 and 6 m overlapped with the latter (Figure 3b). The respiration rates showed a congruent pattern. When normalized to FM, rates were highest at 4 m with -2.9 ± 0.4 µmol $O_2 \cdot g^{-1}$ FM· h^{-1} and thereby almost 50% higher than at 2 m, while rates at 0.5 and 6 m were intermediate (Figure 3e; Tukey test: $p < 0.004$). The same general pattern in respiration rates was apparent when normalized to DA (Figure 3e; Tukey test: $p < 0.001$).

Experiment 2 – Blade gradient. The impact of normalization to either FM or DA on Chl *a* and photosynthetic parameters measured along the blade gradient from the base to the tip of 2-m and 4-m algae is exhibited in Figures 4 and 5, respectively. Normalization to FM resulted in significant differences in Chl *a*, P_{max}, and α along the blade gradient. Respiration rates also showed large but insignificant increases. In contrast,

normalization to DA resulted in stable values along the blade gradient in all photosynthetic parameters, but not for the Chl *a* content (Table 4). The interaction of factor depth × blade region was tested for all parameters, revealing no significant effect (statistics not shown).

Blade region had an overall significant effect on the Chl *a* content irrespective of the used normalization parameter (Table 4). At 2 m depth, Chl *a* of FM of distal discs was 36% higher than that of medial discs (Figure 4a), but differences were not significant due to the lowered *p*-value after Bonferroni-correction (α = 0.017; Tukey test: $p < 0.03$). At 4 m depth, Chl *a* of FM of distal discs was 0.05 ± 0.01 mg· g^{-1} FM and thereby 35% higher than in the basal region (Figure 4d; Tukey test: $p < 0.007$). Chl *a* at DA at 2 and 4 m depth showed the opposite pattern. There was a significantly higher Chl *a* at DA content in basal discs compared to medial and distal discs at 2 m (basal: 0.01 ± 0.003 mg· cm^{-2} DA; medial:

TABLE 3 Results of one-factorial ANOVAs along the depth gradient.

Parameter	df	DA		FM	
		F	p	F	p
Chl a	3	2.69	0.074	1.89	0.164
I_c	3	3.41	**0.037**	3.55	**0.033**
I_k	3	1.12	0.366	1.46	0.256
P_{max}	3	1.99	0.148	1.58	0.226
R	3	7.73	**0.001**	6.17	**0.004**
α	3	0.02	0.997	0.02	0.997

Note: Effect of depth (0.5, 2, 4 and 6 m) on chlorophyll *a* concentration (Chl *a*) and photosynthetic parameters calculated from PI curves modeled after Jassby and Platt (1976) of *Laminaria hyperborea* blade discs (*n* = 6), which were normalized to either disc area (DA) or fresh mass (FM). Significant effects are in bold (α = 0.05).

0.007 ± 0.002 mg · cm^{-2} DA; distal: 0.008 ± 0.001 mg · cm^{-2} DA; Figure 4a; Tukey test: $p < 0.003$) and in basal compared to distal discs at 4 m (basal: 0.014 ± 0.009 mg · cm^{-2} DA; distal: 0.001 ± 0.006 mg · cm^{-2} DA; Figure 4d; Tukey test: $p < 0.001$).

There were no significant differences of the reference independent parameters I_c and I_k along the blade gradient (Figure 4b,c,e,f). At 2 and 4 m depths, I_c was 5.8 ± 3.6 µmol photons · m^{-2} · s^{-1} and 13.0 ± 7.8 µmol photons · m^{-2} · s^{-1}, respectively, showing two- to three-fold higher values at 4 m than those at 2 m (Figure 4b,e; Table 4). Similarly, I_k was stable at basal, medial, and distal discs, with an I_k of 69.4 ± 13 µmol photons · m^{-2} · s^{-1} at 2 m (Figure 4c) and of 70.5 ± 15.9 µmol photons · m^{-2} · s^{-1} at 4 m (Figure 4f; Table 4). There were no significant differences in respiration rates for both depths and reference parameters along the blade gradient. Respiration rates normalized to FM decreased considerably between the basal and the distal region (Table 4; Figure 5b,e). Only when normalized to FM was P_{max} significantly different along the blade gradient for both depths (Table 4; Figure 5a). Lowest values were in the basal region, which increased significantly in the distal region by 52% to 26.7 ± 3.7 µmol O$_2$ · g^{-1} FM · h^{-1} at 2 m and by 50% to 20.6 ± 3.1 µmol O$_2$ · g^{-1} FM · h^{-1} at 4 m (Figure 5a,d; Tukey test: $p < 0.011$). Similarly, the light utilization coefficient α at 2 m was not significantly different along the blade gradient when normalized to DA but increased significantly from the basal to distal region when normalized to FM (Figure 5c; Table 4; Tukey test: $p < 0.005$). The basal region had a low α of 0.2 ± 0.03 µmol O$_2$ · g^{-1} FM · h^{-1} (µmol photons · m^{-2} · s^{-1})$^{-1}$, which nearly doubled in the distal region with 0.4 ± 0.05 µmol O$_2$ · g^{-1} FM · h^{-1} (µmol photons · m^{-2} · s^{-1})$^{-1}$. At 4 m, the general pattern in α was the same for both reference parameters, but differences in FM normalized data were not significant (Figure 5f; Table 4).

Underwater light climate

Recorded underwater PAR at four different depths (1.2, 2.9, 4.4, and 6.6 m) showed periods of low turbidity and high incident irradiance in July and the beginning of August as well as highly turbid periods with low incident irradiance in August and September (Figures 6 and 7a–c). During the sampling period, several storm events with cloudy skies and high wind speeds were observed, causing increased water turbidity. Consequently, measured incident PAR at the water surface (Land Station Helgoland, COSYNA data web portal: http://codm. hzg.de/codm/), measured at noon, largely varied between 365 µmol photons · m^{-2} · s^{-1} (17 August, 2014) and 1778 µmol photons · m^{-2} · s^{-1} (19 July, 2014). PAR values, measured at noon at 1.2 m depth, ranged from 13 µmol photons · m^{-2} · s^{-1} (10 August, 2014) to 866 µmol photons · m^{-2} · s^{-1} (19 July, 2014; Figure 6a, c). Figure 6 highlights the large differences in calculated hourly K$_d$ (PAR) between a cloud-free, calm day with a mean value of 0.42 ± 0.03 m^{-1} (19 July; Figure 6b), showing only small hourly variations during the entire photoperiod, and an overcast and stormy day with a K$_d$ (PAR) of 0.75 ± 0.23 m^{-1} (10 August; Figure 6d) and a large variability in hourly values. Calculated daily K$_d$ (PAR) was lowest and between 0.28 m^{-1} with a 95% confidence interval (CI) of 0.25–0.31 m^{-1} (range of hourly K$_d$ (PAR)) on 7 September and highest with 0.87 m^{-1} with a CI of 0.77–0.97 m^{-1} on 11 August (Figure 7c). The mean daily K$_d$ (PAR) was 0.46 m^{-1} for the entire sampling period (Figure 7c).

Modeled net primary production of the *Laminaria hyperborea* forest

The modeled daily net C-fixation rates over the depth gradient between 0 and 6.6 m are exhibited in Figure 7d. The figure shows that production over summer was highly variable and that periods with high K$_d$ values, indicating increased turbidity after storm events (Figure 7c), led to a negative carbon balance in depths below 3–4 m MLWS over several weeks, although incident PAR was not low (Figure 7a). Based on daily K$_d$ values, highest daily NPP were calculated for cloud-free, calm days ranging between 3.5 ± 0.8 g C · m^{-2} seafloor · d^{-1} at 2 m and 1 ± 0.2 g C · m^{-2} seafloor · d^{-1} at 6 m on 19 July. Lowest daily NPP was calculated during a stormy period on 17 August, ranging between 0.62 ± 0.3 g C · m^{-2} seafloor · d^{-1} at 0.5 m and −0.45 ± 0.1 g C · m^{-2} seafloor · d^{-1} at 6 m. Interestingly, NPP of *Laminaria hyperborea* at 2 m depth was 22% higher than at 0.5 m during calm periods between 2 and 8 August. Averaging daily NPP over each investigated depth and over the entire 7 weeks resulted in mean daily summer NPP of *Laminaria* of 2.1, 2.3, 1.2 and 0.2 g C · m^{-2} seafloor · d^{-1} at 0.5, 2, 4, and 6 m, respectively (Table 5). Using these
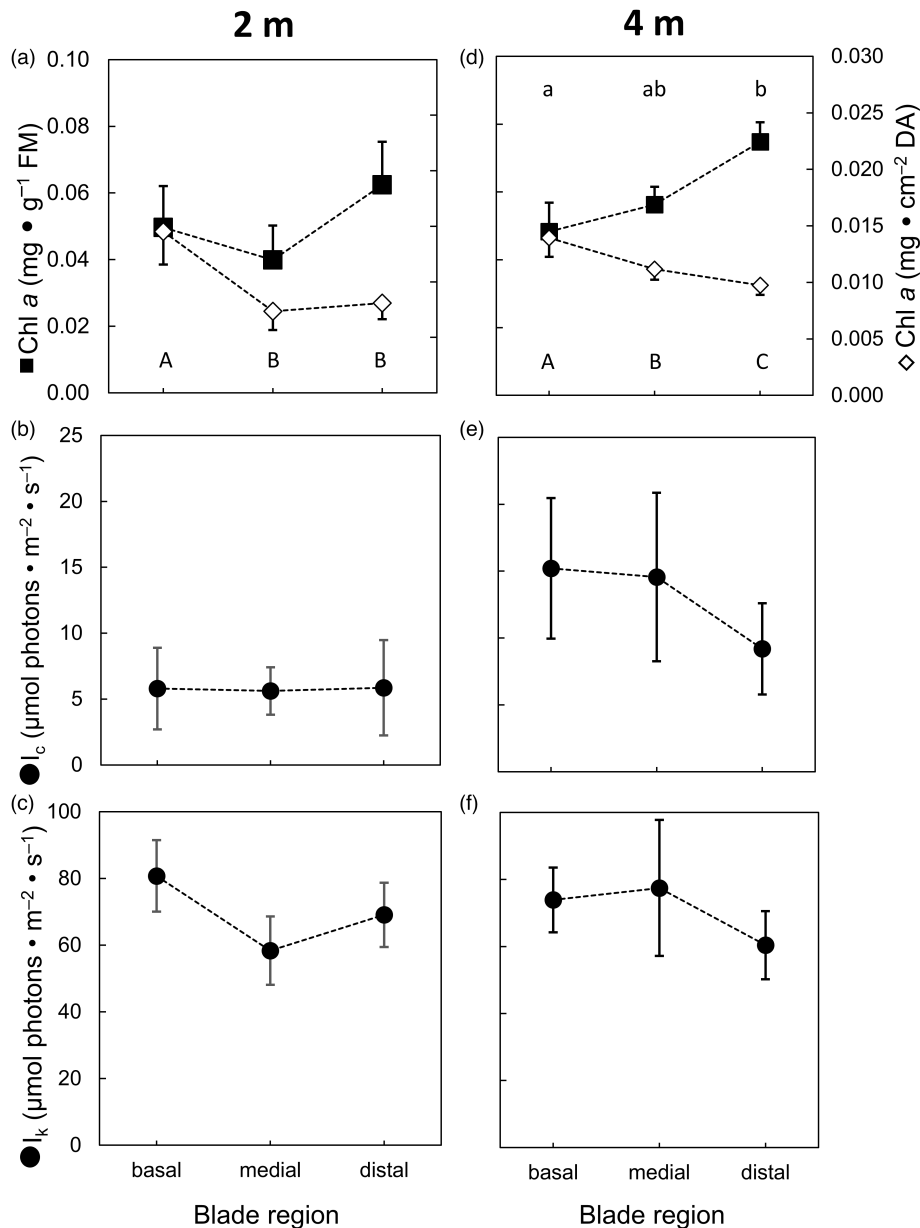
FIGURE 4 Chlorophyll a concentration (Chl a), light saturation point (I_k), and light compensation point (I_c) along the blade gradient of *Laminaria hyperborea* ($n = 6$ each blade region) collected at 2 and 4 m. Blade regions were cut 5 cm (basal), 25 cm (medial), and 50 cm (distal) above the stipe-blade transition zone. (a) and (d) Chl a was normalized to either fresh mass (FM; black square) or disc area (DA; white diamond). Units of (b) and (e) I_c and (c) and (f) I_k are independent from normalization and the same for both reference parameters (filled circles). Lower case and capital letters within each subplot show significant differences between regions related to either FM or DA, respectively (Statistical results: Table 4).

mean values, mean summer NPP of the whole kelp forest was 1.5 ± 0.97 g C$\cdot$m^{-2} seafloor$\cdot$d^{-1}.

Furthermore, the mean, minimum, and maximum daily K_d values of 0.46, 0.28, and 0.87 m^{-1}, respectively, were used to calculate daily NPP rates (hereafter called NPP) for the different depths during the entire sampling period. Results were compared to the estimated NPP based on daily K_d (NPP$_{\text{daily Kd}}$; Tables 5 and S2 in the Supporting Information). Although mean values were quite different, overall summer NPP at all four depths revealed no significant

differences between the four different NPP calculations (NPP$_{\text{daily Kd}}$, NPP$_{\text{mean Kd}}$, NPP$_{\text{min Kd}}$, NPP$_{\text{max Kd}}$; t-test: NPP$_{\text{mean Kd}}$: $T = -1.7$, df $= 4$, $p = 0.2$; NPP$_{\text{min Kd}}$: $T = -2.2$, df $= 4$, $p = 0.1$; NPP$_{\text{max Kd}}$: $T = 1.6$, df $= 4$, $p = 0.1$). The coefficient of determination was higher when relating NPP$_{\text{daily Kd}}$ and NPP$_{\text{mean Kd}}$ ($R^2 > 0.93$), than relating NPP$_{\text{daily Kd}}$ and either NPP$_{\text{min Kd}}$ or NPP$_{\text{max Kd}}$ ($R^2 < 0.88$ and $R^2 < 0.76$, respectively; Table 6). Separated by depth, the comparison of NPP based on different K_d values revealed significant differences only at 4 and 6 m (Table 7). For 0.5 and
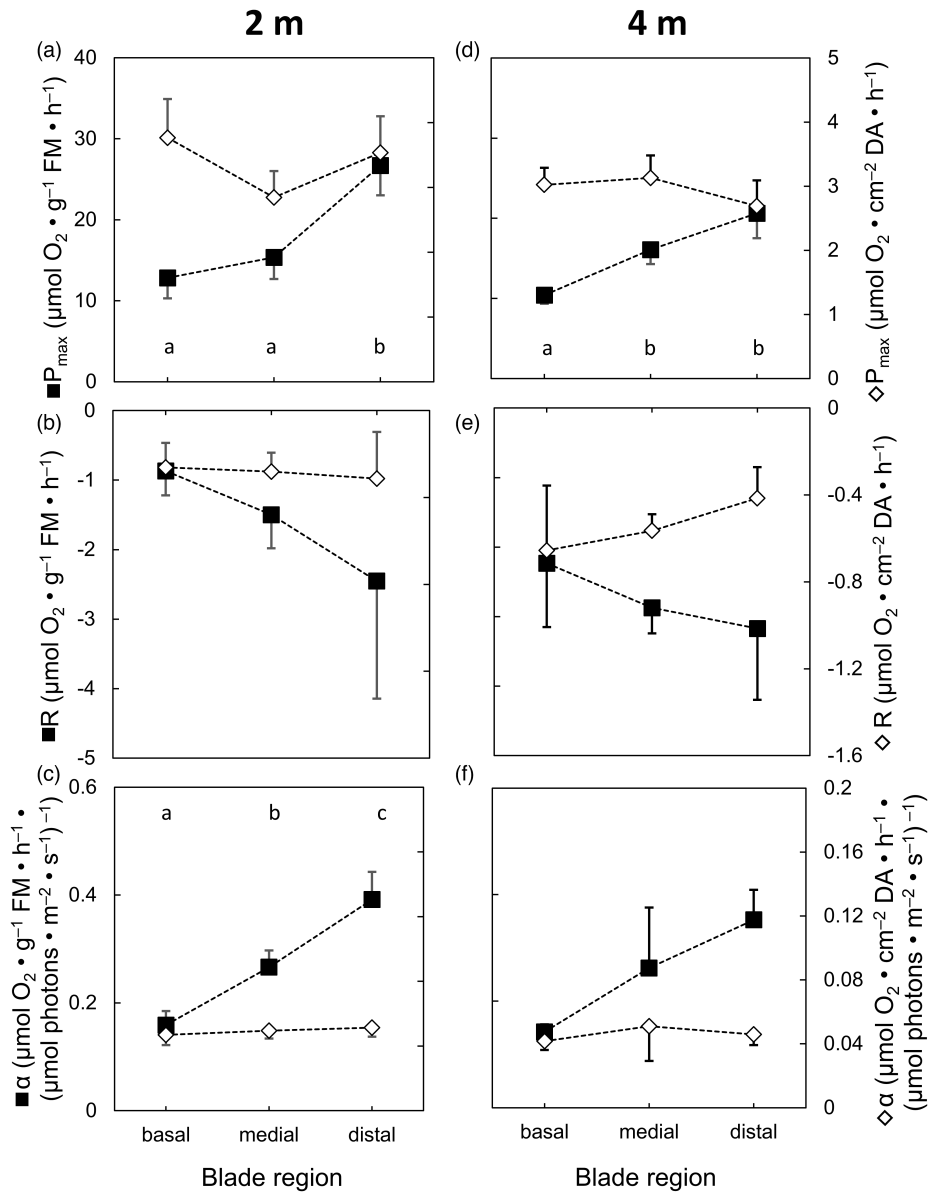
FIGURE 5 Photosynthesis versus irradiance (PI) parameters along the blade gradient of *Laminaria hyperborea* ($n = 6$ each blade region) collected at 2 and 4 m. Blade regions were cut 5 cm (basal), 25 cm (medial), and 50 cm (distal) above the stipe-blade transition zone. PI parameters (a), (d) P_{max}, (b), (e) R, (c), and (f) α were normalized to either fresh mass (FM; black square) or disc area (DA; white diamond). Lower case and capital letters within each subplot show significant differences between regions related to either FM or DA, respectively (Statistical results: Table 4).

2 m, the coefficient of determination was $R^2 > 0.93$, while at 4 and 6 m depth R^2 was <0.88 and <0.80, respectively (Table 6). $NPP_{daily\ Kd}$ was not significantly different to $NPP_{mean\ Kd}$ (post hoc Test: 4 m $p = 0.73$, 6 m $p = 0.9$; Table S3 in the Supporting Information). At 4 m, $NPP_{daily\ Kd}$ was significantly lower by −38% than $NPP_{min\ Kd}$ (post hoc Test: $p = 0.008$) and significantly higher by 107% than $NPP_{max\ Kd}$ (post hoc Test: $p < 0.001$; Tables 5 and S3). At 6 m, $NPP_{daily\ Kd}$ was significantly lower by −69% than $NPP_{min\ Kd}$ (post hoc Test: $p < 0.001$) and significantly higher by 286% than $NPP_{max\ Kd}$ (post hoc Test: $p < 0.001$; Tables 5 and S3).

DISCUSSION

The present study investigated the photosynthetic performance and Chl *a* content of the dominant subtidal NE-Atlantic kelp forest-forming species, *Laminaria hyperborea*, along its depth distribution and along the blade gradient as well as the influence of photosynthetic normalization parameters and variable underwater irradiance for NPP modeling. Although, some data were available about the photosynthetic performance of *L. hyperborea*, the data often lacked the depth or blade gradient component (Küppers & Kremer, 1978; Miller III et al., 2009; Steinbiss & Schmitz, 1974; White

TABLE 4 Results of one-factorial RM ANOVAs of *experiment 2 – blade gradient* separated by depth (2 and 4 m).

	df	Chl a		I_c		I_k		P_{max}		R		α	
		F	p	F	p	F	p	F	p	F	p	F	p
FM													
2 m	2	7.1	**0.012**	0.01	1	4.5	0.04	22.5	**<0.001**	2.7	0.1	62	**<0.001**[a]
4 m	2	12.7	**0.002**	1	0.4	0.9	0.4	14	**0.001**	0.7	0.5	4.2	0.09[a]
DA													
2 m	2	28.2	**<0.001**	0.01	1	4.5	0.04	2.8	0.1	0.2	0.9	0.9	0.4
4 m	2	34.6	**<0.001**	1	0.4	0.9	0.4	1	0.4	1	0.4	0.3	0.7

Note: The effect of blade gradient (5, 25 and 50 cm) on chlorophyll a concentration (Chl a) and photosynthesis versus irradiance parameters of *Laminaria hyperborea* blade discs ($n = 6$ each region), which were normalized either to disc area (DA) or disc fresh mass (FM). Bonferroni-corrected significant differences ($p < 0.017$) is shown in bold.

[a]Greenhouse–Geisser correction.

et al., 2021), which had received some attention in the studies of *Macrocystis* and *Ecklonia* (e.g., Fairhead & Cheshire, 2004; Koch et al., 2016; Rodgers & Shears, 2016).

Brown algae display large differences in the anatomic structure along the thallus, which have a large impact on PI parameters used in NPP models (King & Schramm, 1976). In the present study, it became evident that normalization of photosynthetic parameters to blade area generates more robust data than normalization to fresh mass. Thus, up-scaling of ex situ measurements to in situ demographic kelp parameters via kelp blade area is more reliable than via kelp fresh mass. Photosynthetic rates of seaweeds have to be normalized, and this is achieved via referring to either FM or dry mass or tissue area or Chl a (e.g., Blain et al., 2020; Borlongan et al., 2019; Gévaert et al., 2011; Gómez et al., 2007). Previously, Gévaert et al. (2011) compared oxygen production rates measured in basal discs and whole sporophytes that were either normalized to fresh mass or surface area. They observed comparable oxygen production rates for discs and entire sporophytes only when rates were normalized to surface area (Gévaert et al., 2011). Especially in kelps with their complex tissue, FM decreases toward the distal region (e.g., Krüger, 2016). This change in blade thickness is caused by the increased proportion of non-photosynthetically but respiratory active inner cell layers (cortex and medulla) in the basal region (Kain & Jones, 1976; Steinbiss & Schmitz, 1974). Thus, it was not surprising that in the presented study, FM of thallus discs, and Chl a normalized to FM, displayed a clear gradient along the blade with decreasing disc FM and increasing disc Chl a from the basal to the distal region. In contrast, disc FM and Chl a taken at the same blade location (25 cm) along the depth gradient were not significantly different irrespective of normalization to either FM or DA. That, too, was to be expected, as at comparable blade locations the same thallus thickness and structure is expected (Kain & Jones, 1976; Steinbiss & Schmitz, 1974).

Within the complex thallus of brown algae, all cells contain plastids, but well-developed highly pigmented chloroplasts are present in cells of the outer cell layers of the meristoderm and cortex rather than in the medulla, and thereby, the medulla plays a minor role in photosynthesis (Garbary & Kim, 2005; Grevby et al., 1989). Presumably, this general anatomical pattern does not change much along the blade gradient. Hence, due to the higher proportion of photosynthetically inactive medulla cells lacking pigments (personal observation of K. Franke; Garbary & Kim, 2005), Chl a normalized to FM significantly increased from the basal to the distal region, while Chl a normalized to DA showed a reverse pattern. The observed slightly higher Chl a content in the basal region when normalized to DA may be a result of reduced in situ irradiances at
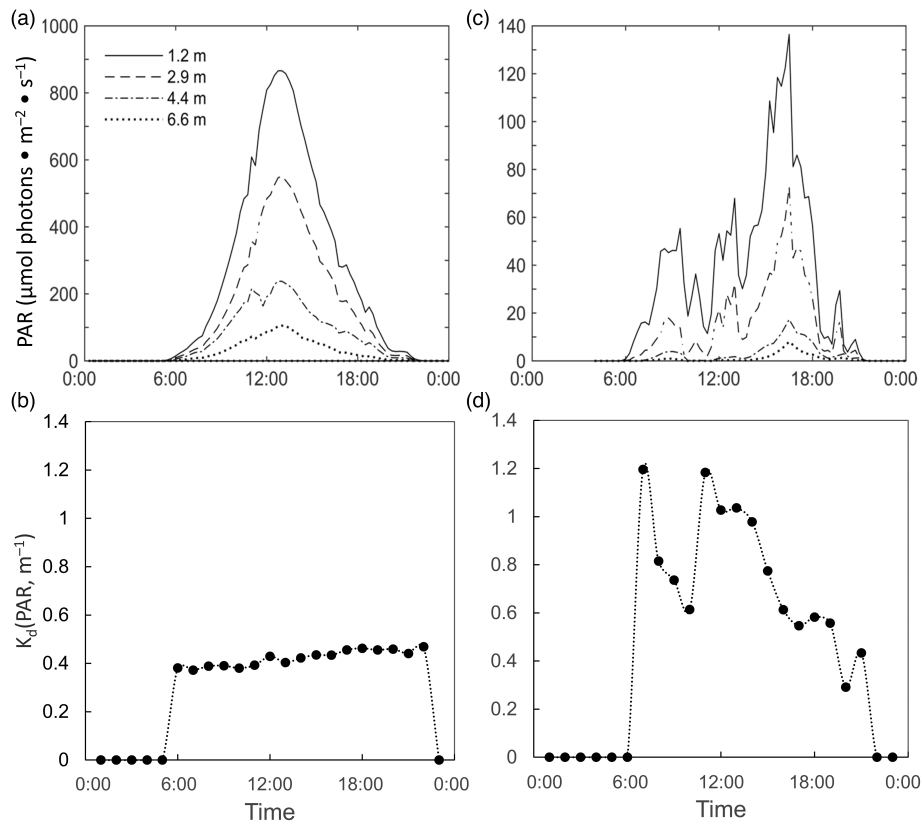
FIGURE 6 Underwater light availability of two different days. Hourly photosynthetically active radiation (PAR) for (a) 19 July and (c) 10 August 2014 measured at four depths (1.2, 2.9, 4.4, and 6.6 m), and hourly K_d(PAR), calculated over the depth gradient, for (b) 19 July (calm and sunny day) and (d) 10 August, 2014 (stormy and cloudy day).

the basal blade meristem compared to distal parts at the light-flooded kelp forest canopy, leading to an increase in Chl *a* contents under low light conditions (Buschmann et al., 2014; Kirk, 1994).

When normalized to FM, PI parameters P_{max} and α also increased from basal to distal regions for the same reason of a relatively higher ratio of structural to photosynthetic tissues, which tend to have a lower photosynthetic capacity than the distal regions (Littler & Littler, 1980; Steinbiss & Schmitz, 1974). Surprisingly, respiration rates normalized to FM were not significantly different along the blade, although values were more variable compared to respiration rates normalized to DA. Measured PI parameters normalized to DA displayed no significant trends. In conclusion, these results highlight the importance of carefully considering the reference parameter when interpreting existing data on photoacclimation of kelp (Andersen et al., 2013; Gerard, 1986, 1988; Pedersen et al., 2014). To convert published photoacclimation parameters with different normalization parameters, we provide DM:FM ratios as well as DM:area ratios (Table S4 in the Supporting Information), which are comparable to previously published ratios of *Laminaria hyperborea* sporophytes off Helgoland (Lüning, 1979).

In contrast to the pronounced differences along the blade gradient, most PI parameters and Chl *a* content of *Laminaria hyperborea* blades remained stable along

the depth gradient, independent of the reference parameter. Only the light compensation point I_c and respiration rates differed, but without displaying a significant trend and without a reasonable explanation for these differences. Overall, measured respiration rates normalized to FM were comparable to published respiration rates of *L. hyperborea*, ranging between −23.4 and −5.63 μmol $O_2 \cdot g^{-1}$ DM$\cdot h^{-1}$ with lowest values measured when the entire algae were incubated (Duarte et al., 2013; Johansson & Snoeijs, 2002; Lüning, 1979). Respiration rates normalized to DA were comparable to respiration rates of *L. digitata*, sampled in Roscoff, France and Wissant, England (Delebecq et al., 2013). Presented in vitro PI parameters are in the range of previously reported values (Lüning, 1979; Miller III et al., 2009; White et al., 2021); however, differences in the age of algae (Altamirano et al., 2003; Campbell et al., 1999), sampling season (Dunton & Schell, 1986; Fairhead & Cheshire, 2004; Marambio et al., 2017), water temperatures (Kain, 1979; Machalek et al., 1996; Pedersen et al., 2014), and experimental set-up and reference parameters (Gévaert et al., 2011; Johansson & Snoeijs, 2002; Krüger, 2016) can lead to large variations in PI parameters.

Our study furthermore showed that underwater irradiance is extremely variable even over one season in coastal waters, in our case summer 2014, and thereby
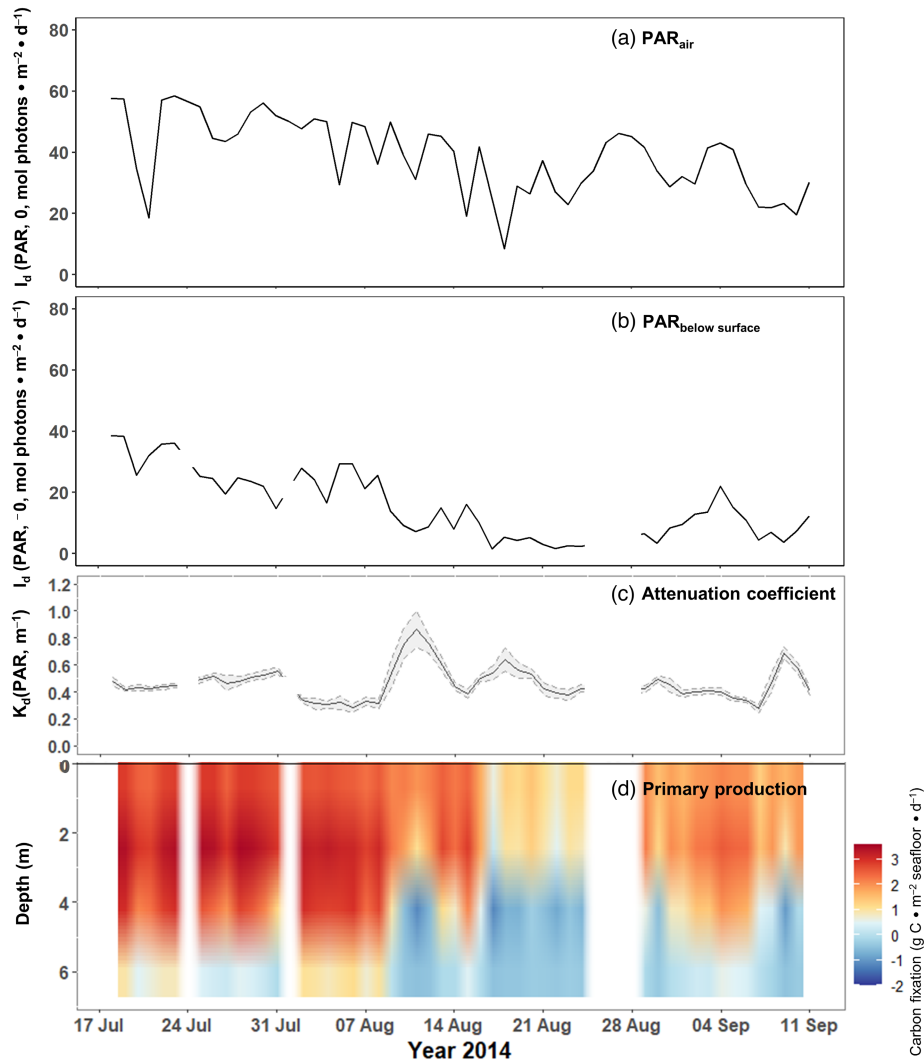
FIGURE 7 Summer incident irradiance and daily net primary production (NPP) rates of the *Laminaria hyperborea* forest surrounding Helgoland between 0 and 6.6 m water depth. Incident irradiance is shown for (a) daily integrated photosynthetically active radiation at the water surface I_d (PAR, 0) during the sampling period (Land Station Helgoland, COSYNA data web portal: http://codm.hzg.de/codm/). (b) Daily integrated PAR just below the water surface I_d (PAR, 0^-) was estimated with calculated hourly K_d(PAR) and in situ I_d (z_2) at $z_2 = 1.2$ m over the entire sampling period. (c) The mean vertical diffuse vertical attenuation coefficient K_d (PAR) (black line) is shown with 95% confidence interval (gray). (d) Calculated daily NPP for all four investigated depths is given as carbon fixation rate per square meter seafloor and was interpolated along the entire vertical profile. Missing data are represented as white areas in all subplots. [Color figure can be viewed at wileyonlinelibrary.com]

TABLE 5 Net primary production (NPP, g C · m^{-2} seafloor · d^{-1}) based on photosynthetic versus irradiance curve parameters and photosynthetically active radiation (PAR).

Depth (m)	NPP$_{daily}$ K_d	NPP$_{mean}$ K_d	NPP$_{min}$ K_d	NPP$_{max}$ K_d
	(g C · m^{-2} seafloor · d^{-1})			
0.5	2.12 ± 0.61	2.16 ± 0.61	2.12 ± 0.62	2.25 ± 0.57
2	2.34 ± 0.18	2.42 ± 0.16	2.55 ± 0.16	2.11 ± 0.16
4	1.24 ± 1.40	1.35 ± 1.20	2.01 ± 1.21	−0.09 ± 0.82
6	0.21 ± 0.51	0.18 ± 0.38	0.67 ± 0.52	−0.39 ± 0.07
Overall mean	1.48 ± 0.97	1.53 ± 1.01	1.84 ± 0.81	0.97 ± 1.40

Note: PAR along the vertical depth profile was calculated with different diffuse vertical attenuation coefficients (K_d) calculated either for each day (daily K_d), mean daily K_d over the 7 weeks, lowest daily K_d (minimum K) or highest daily K_d (maximum K_d) measured during the 7 weeks. Additionally, the overall mean for all four depths is shown. Statistical results are shown in Tables 7 and S4 in the Supporting Information.

considerably influences estimations of daily or annual net primary production rates. Similar underwater irradiance variations have been shown elsewhere (e.g., Dean, 1985; Dunton, 1990). As the recently observed increase in turbidity of coastal waters called "coastal darkening" (e.g., Capuzzo et al., 2015) can negatively affect kelp production (Blain et al., 2021; Mabin et al., 2019), a thorough discussion of light input into production models is thus of utmost importance.

The interpretation of our data should be considered under the constraints of the sample size and the sampling schedule. Our sample size of $n = 6$ is relatively high for physiological photosynthesis studies compared to similar other studies (e.g., Deregibus et al., 2016: $n = 4$; Gévaert et al., 2003: $n = 3$; Gómez et al., 1997: $n = 4$; Hanelt, 1998: $n = 3$; Pedersen et al., 2014: $n = 3$). Our study even accounted for the diurnal variation of photosynthetic activity (Granbom et al., 2001; Henley et al., 1991; Schubert et al., 2004) by measuring 50% of the replicates in the morning and 50% in the afternoon, thereby gaining a robust mean value of the daily performance. However, the sampling schedule may have induced an unforeseen bias as samples from different depths were taken within a period of 7 weeks and samples for the blade gradient experiment were taken several days apart from each other. In the latter case, care was taken so that at each time point the full blade gradient was measured from two individuals. Thereby, mean values integrate a potential impact of time on the response values. During the experimental period, very variable in situ irradiance conditions were monitored due to stormy and turbid phases. Hence, in situ photoacclimation to increased turbidity and high stress levels may have induced a differential pre-conditioning. In addition, many of the kelp individuals showed at least some epizoic bryozoan cover. Beside these changing

light climateic conditions, summer surface water temperatures of $18 \pm 2°C$ were near the reported 2-week survival temperature of sporophytes of Helgolandic *Laminaria hyperborea* at 20–21°C (tom Dieck, 1992). A study on *Saccharina latissima* showed that photosynthesis was not affected by a temperature fluctuation of 2–3°C. Oxygen production rates were comparable between algae grown at an optimal temperature of 15 and 18°C for 3 weeks and a sub-lethal temperature of 20°C for 1 week (Gerard & Du Bois, 1988). Thus, the short-term temperature fluctuation during the experimental period most likely had no effect on photosynthesis.

As an overall conclusion, we are confident that the obtained values sufficiently characterize the summer situation at our study location, especially as the general lack of changes in photosynthetic parameters of *Laminaria hyperborea*, as well as of *Saccharina latissima*, along a depth gradient or at different light levels has been shown earlier (Lüning, 1979, 1981; Machalek et al., 1996); thus, the lack of changes may not have been induced by our sampling design. These observations indicate a high photoacclimation potential and/or a high recovery potential of kelp species toward varying light availability. The lack of photoinhibition observed in our laboratory conducted PI-curves for individuals from all four depths supports the possibility of a high physiological plasticity allowing *L. hyperborea* to grow across the complete upper subtidal zone.

Nevertheless, light availability has been identified as the restricting factor for the depth distribution of *Laminaria hyperborea* (Lüning, 1990), which is located between 1 and 12.5 m water depth in the sublittoral off Helgoland (Pehlke & Bartsch, 2008). Due to a large daily tidal range of nearly 2.5 m (Lüning, 1990) and frequent weather events with strong winds and wave motion, large amounts of sediment can be re-suspended into the water column, which increases light attenuation. We showed a three times higher daily K_d (PAR) during storm events compared to calm days with little wave motion, within a short period in summer. This large variability in daily mean K_d (PAR) values between 0.28 and 0.87 m^{-1} matches previous Secchi disc measurements performed from research vessels between 1979 and 1994 in a 5 km radius around Helgoland (Aarup, 2002). These surveys obtained K_d (PAR) values between 0.25 and 1.48 m^{-1} and were calculated by dividing Secchi disc depth by a factor of 1.48 (Lee et al., 2018). So far, only few annual optical data about turbid coastal

TABLE 6 Coefficient of determination (R^2) between modeled daily net primary production rates (NPP) based on daily diffusion vertical attenuation coefficient (K_d) and modeled daily NPP based on mean, minimum, or maximum daily K_d.

Depth (m)	R^2 (mean K_d)	R^2 (min K_d)	R^2 (max K_d)
0.5	0.962	0.959	0.964
2	0.943	0.938	0.948
4	0.877	0.833	0.872
6	0.793	0.716	0.788
All depths	0.939	0.873	0.755

TABLE 7 Results of different Kruskal–Wallis ANOVAs, one per each depth.

Depth (m)	0.5			2			4			6		
	H	df	*p*	*H*	df	*p*	*H*	df	*p*	*H*	df	*p*
	1.9	3	0.58	6.5	3	0.09	58.4	3	**<0.001**	103.6	3	**<0.001**

Note: Net primary production rates (NPP) calculated from different diffuse vertical attenuation coefficients (K_d) were compared (Table S2). Significance level: $p < 0.05$; each depth $n = 50$.

systems such as the sublittoral off Helgoland or at sites influenced by glacial melt in the Arctic have been published (Hanelt et al., 2001; Lüning & Dring, 1979). Many studies only used short-term continuous underwater irradiance measurements for NPP estimation at other locations (e.g., Dean, 1985; Dunton, 1990, 1994) as logistics to pertain continuous underwater irradiance measurements are high. Meanwhile, several initiatives have started continuous long-term underwater irradiance measurements, e.g., at Helgoland, in the Arctic (CTD2 Underwater Node Helgoland and CTD 90 M Underwater Node Spitsbergen, COSYNA data web portal: http://codm.hzg.de/codm/) or in Potter Cove, Antarctica in the Southern Ocean (Deregibus et al., 2016).

As shown in the present study, K_d (PAR) values are highly variable during one season and always vary diurnally, and hence, single underwater irradiance measurements can lead to large under- or overestimations of NPP as they represent only a snapshot. Our net primary production rates resulted in comparable NPP rates when either daily K_d or mean K_d were used to calculate light input, both based on continuous underwater measurements. However, usage of single minimum K_d values representative of a clear and sunny summer day or maximum K_d values representative of windy conditions resulted in considerable over- or underestimation of NPP, especially in depths ≥4 m. To determine a representative mean daily K_d of the investigated season for reliable NPP estimations without performing daily underwater light measurements, we propose a weighted mean K_d (Matthes et al., 2021; Equation 2). A weighted average takes into account the weight or, in this application, frequency of high and low daily K_d values during the sampling period. To separate calm days with a low daily K_d from stormy days with a high K_d, we used a threshold of daily averaged wind speed of 8 m·s^{-1}, which is equivalent to 16 knots or number 4 (moderate breeze) on the Beaufort scale. According to the Beaufort scale, above number 4, the wave heights increase >1.83 m with many white caps. Although this wind speed threshold is believed to be applicable for several coastal regions with shallow kelp forests, the threshold should be adjusted for different local conditions and deeper kelp forests. Helgoland daily averaged wind speed data for our study period was downloaded from the open-access database of the German weather service (Deutscher Wetterdienst, https://www.dwd.de/DE/leistungen/klimadatendeutschland/klarchivtagmonat.html?nn=16102). The weighted mean K_d was calculated using the ratio of calm days and stormy days, respectively to the number of days in the sampling period (total days) as follows:

$$0.47\,\text{m}^{-1} = \frac{21}{50} \cdot 0.42\,\text{m}^{-1} + \frac{29}{50} \cdot 0.50\,\text{m}^{-1}$$

For our study period, the calculated weighted mean daily K_d of 0.47 m^{-1} is close to the mean daily K_d of 0.46 m^{-1}, when averaging all daily K_d measurements of the sampling period. These results show that a weighted seasonal K_d of vertical light measurements during different weather conditions provides a useful alternative to continuous underwater light measurements. This is preferred over single light measurements at fixed days or times of the day (e.g., only midday) or using seasonal averages of irradiance values (Anthony et al., 2004; Pedersen et al., 2014), which may possibly lead to large uncertainties and inaccuracies in NPP estimations. Unexpectedly, during several days in mid-August 2014, PAR was close to zero at 6.6 m depth during the day, which led to a temporal negative C-balance of *Laminaria hyperborea* >3–4 m. Although daily C-fixation rates per cm^2 DA where highest in blades at 0.5 m water depth, highest daily C-fixation rates per m^2 seafloor were calculated for blades between 2 and 4 m due to the multiplication of rates with blade area per m^2 seafloor. The biomass maximum of *Laminaria* around Helgoland is at 4 m depth (Pehlke & Bartsch, 2008; Steinberg, 2019). Only during stormy periods in August and September, maximum production of *L. hyperborea* shifted to the surface due to decreased PAR levels at greater depths.

PI parameters gained in oxygen incubation experiments in combination with in situ continuous PAR measurements, known LAI, and a PQ of 1.18 was used to calculate for the first time a depth integrated mean daily summer NPP of 1.5 ± 0.97 g C· m^{-2} seafloor· d^{-1} of *Laminaria hyperborea* for the summer period. So far, only a few PQ-values are known for *L. hyperborea,* and kelp in general (Gerard, 1988; Iñiguez et al., 2016; Miller III et al., 2009). Iñiguez et al. (2016) calculated PQ-values for kelp species that were exposed to different temperatures in combination with different carbon dioxide levels, showing no significant influence of these factors, but all PQ values were species-specific. However, it is still unclear how PQs are influenced by season and depth. In this study, modeled NPP was comparable to estimated NPP of other *L. hyperborea* forests along European coastlines ranging from 0.5–13.3 g C· m^{-2} seafloor· d^{-1} (Kain & Jones, 1977; Smale et al., 2020; White et al., 2021). Although the Helgolandic *L. hyperborea* forest is relatively small compared to kelp forests along the British and Norwegian coastlines, our NPP calculation demonstrated that it is a very productive ecosystem in the southern North Sea, which presumably strongly influences the surrounding soft bottom areas

$$\text{Weighted daily } \overline{K_d} = \frac{\text{No. calm days}}{\text{No. total days}} \cdot \text{daily } \overline{K_{d,\text{calm days}}} + \frac{\text{No. stormy days}}{\text{No. total days}} \cdot \text{daily } \overline{K_{d,\text{stormy days}}} \tag{6}$$

by a considerable carbon export as was shown in detail for other regions (e.g., Krumhansl & Scheibling, 2012; Pedersen et al., 2020), but its CO_2 capture potential will be strongly dependent on future storm activity and water clarity as was shown here.

Most recently, Duarte et al. (2022) compiled the scattered information on NPP rates in macroalgal habitats around the globe and estimated the global extent of macroalgal habitats. This resulted in a global macroalgal NPP model, although global NPP values for macroalgae are still prone to high insecurities and variations that even became apparent in our detailed local study. CO_2 uptake, standing stock, and carbon export of kelp forests are likely to change under global climate change, highlighting the urgent need to quantify and investigate processes that lead to regional differences in standing stock and biomass accumulation for a better understanding of regional and global marine carbon cycles.

AUTHOR CONTRIBUTIONS

Kiara Franke: Conceptualization (equal); data curation (lead); formal analysis (lead); methodology (equal); validation (lead); visualization (lead); writing – original draft (lead); writing – review and editing (lead). **Lisa C. Matthes:** Conceptualization (lead); data curation (lead); formal analysis (equal); investigation (lead); methodology (lead); validation (lead); visualization (lead); writing – original draft (lead); writing – review and editing (equal). **Angelika Graiff:** Conceptualization (equal); formal analysis (equal); writing – original draft (equal); writing – review and editing (equal). **Ulf Karsten:** Conceptualization (equal); formal analysis (equal); writing – original draft (equal); writing – review and editing (equal). **Inka Bartsch:** Conceptualization (lead); formal analysis (equal); methodology (lead); project administration (lead); resources (lead); supervision (lead); writing – original draft (equal); writing – review and editing (equal). The two main authors (KF and LM) contributed the same amount to this manuscript.

ACKNOWLEDGMENTS

ORCID

Kiara Franke https://orcid.org/0000-0001-6318-8475
Lisa C. Matthes https://orcid.org/0000-0002-7362-0417
Angelika Graiff https://orcid.org/0000-0001-8754-6281
Ulf Karsten https://orcid.org/0000-0002-2955-0757
Inka Bartsch https://orcid.org/0000-0001-7609-2149

REFERENCES

Aarup, T. (2002). Transparency of the North Sea and Baltic Sea-a Secchi depth data mining study. *Oceanologia*, *44*, 323–337.

Altamirano, M., Murakami, A., & Kawai, H. (2003). Photosynthetic performance and pigment content of different developmental stages of *Ecklonia cava* (Laminariales, Phaeophyceae). *Botanica Marina*, *46*, 9–16.

Andersen, G. S., Pedersen, M. F., & Nielsen, S. L. (2013). Temperature acclimation and heat tolerance of photosynthesis in Norwegian *Saccharina latissima* (Laminariales, Phaeophyceae). *Journal of Phycology*, *49*, 689–700.

Anthony, K. R. N., Ridd, P. V., Orpin, A. R., Larcombe, P., & Lough, J. (2004). Temporal variation of light availability in coastal benthic habitats: Effects of clouds, turbidity, and tides. *Limnology and Oceanography*, *49*, 2201–2211.

Araujo, R., Barbara, I., Tibaldo, M., Berecibar, E., Tapia, P. D., Pereira, R., Santos, R., & Pinto, I. S. (2009). Checklist of benthic marine algae and cyanobacteria of northern Portugal. *Botanica Marina*, *52*, 24–46.

Assis, J., Lucas, A. V., Bárbara, I., & Serrão, E. Á. (2016). Future climate change is predicted to shift long-term persistence zones in the cold-temperate kelp *Laminaria hyperborea*. *Marine Environmental Research*, *113*, 174–182.

Bidwell, R., & McLachlan, J. (1985). Carbon nutrition of seaweeds: Photosynthesis, photorespiration and respiration. *Journal of Experimental Marine Biology and Ecology*, *86*, 15–46.

Blain, C. O., Hansen, S. C., & Shears, N. T. (2021). Coastal darkening substantially limits the contribution of kelp to coastal carbon cycles. *Global Change Biology*, *27*, 5547–5563.

Blain, C. O., Rees, T. A. V., Hansen, S. C., & Shears, N. T. (2020). Morphology and photosynthetic response of the kelp *Ecklonia radiata* across a turbidity gradient. *Limnology and Oceanography*, *65*, 529–544.

Bolton, J., & Lüning, K. (1982). Optimal growth and maximal survival temperatures of Atlantic *Laminaria* species (Phaeophyta) in culture. *Marine Biology*, *66*, 89–94.

Borlongan, I. A., Maeno, Y., Kozono, J., Endo, H., Shimada, S., Nishihara, G. N., & Terada, R. (2019). Photosynthetic performance of *Saccharina angustata* (Laminariales, Phaeophyceae) at the southern boundary of subarctic kelp distribution in Japan. *Phycologia*, *58*, 300–309.

Buesa, R. J. (1980). Photosynthetic quotient of marine plants. *Photosynthetica*, *14*, 337–342.

Buschmann, A. H., Pereda, S. V., Varela, D. A., Rodríguez-Maulén, J., López, A., González-Carvajal, L., Schilling, M., Henríquez-Tejo, E. A., & Hernández-González, M. C. (2014). Ecophysiological plasticity of annual populations of giant kelp (*Macrocystis pyrifera*) in a seasonally variable coastal environment in the northern Patagonian inner seas of southern Chile. *Journal of Applied Phycology*, *26*, 837–847.

Campbell, S. J., Bite, J. S., & Burridge, T. R. (1999). Seasonal patterns in the photosynthetic capacity, tissue pigment and nutrient content of different developmental stages of *Undaria pinnatifida* (Phaeophyta: Laminariales) in port Phillip Bay, south-eastern Australia. *Botanica Marina*, *42*, 231–241.

Capuzzo, E., Stephens, D., Silva, T., Barry, J., & Forster, R. M. (2015). Decrease in water clarity of the southern and Central North Sea during the 20th century. *Global Change Biology*, *21*, 2206–2214.

Colombo-Pallotta, M. F., García-Mendoza, E., & Ladah, L. B. (2006). Photosynthetic performance, light absorption, and pigment composition of *Macrocystis pyrifera* (Laminariales, Phaeophyceae) blades from different depths. *Journal of Phycology*, *42*, 1225–1234.

Dean, T. A. (1985). The temporal and spatial distribution of underwater quantum irradiation in a southern California kelp forest. *Estuarine, Coastal and Shelf Science*, *21*, 835–844.

Delebecq, G., Davoult, D., Menu, D., Janquin, M. A., Dauvin, J. C., & Gévaert, F. (2013). Influence of local environmental conditions on the seasonal acclimation process and the daily integrated production rates of *Laminaria digitata* (Phaeophyta) in the English Channel. *Marine Biology*, *160*, 503–517.

Deregibus, D., Quartino, M. L., Campana, G. L., Momo, F. R., Wiencke, C., & Zacher, K. (2016). Photosynthetic light requirements and vertical distribution of macroalgae in newly ice-free areas in potter cove, South Shetland Islands, Antarctica. *Polar Biology*, *39*, 153–166.

Duarte, C. M., Gattuso, J. P., Hancke, K., Gundersen, H., Filbee-Dexter, K., Pedersen, M. F., Middelburg, J. J., Burrows, M. T., Krumhansl, K. A., Wernberg, T., & Moore, P. (2022). Global estimates of the extent and production of macroalgal forests. *Global Ecology and Biogeography*, *31*, 1422–1439.

Duarte, P., Ramos, M., Calado, G., & Jesus, B. (2013). *Laminaria hyperborea* photosynthesis irradiance relationship measured by oxygen production and pulse-amplitude-modulated chlorophyll fluorometry. *Aquatic Biology*, *19*, 29–44.

Dunton, K. H. (1990). Growth and production in *Laminaria solidungula*: Relation to continuous underwater light levels in the Alaskan high Arctic. *Marine Biology*, *106*, 297–304.

Dunton, K. H. (1994). Seasonal growth and biomass of the subtropical seagrass *Halodule wrightii* in relation to continuous measurements of underwater irradiance. *Marine Biology*, *120*, 479–489.

Dunton, K. H., & Schell, D. M. (1986). Seasonal carbon budget and growth of *Laminaria solidungula* in the Alaskan high Arctic. *Marine Ecology Progress Series*, *31*, 57–66.

Fairhead, V. A., & Cheshire, A. C. (2004). Seasonal and depth related variation in the photosynthesis–irradiance response of *Ecklonia radiata* (Phaeophyta, Laminariales) at West Island, South Australia. *Marine Biology*, *145*, 415–426.

Garbary, D. J., & Kim, K. Y. (2005). Anatomical differentiation and photosynthetic adaptation in brown algae. *Algae*, *20*, 233–238.

Gerard, V. A. (1986). Photosynthetic characteristics of giant kelp (*Macrocystis pyrifera*) determined in situ. *Marine Biology*, *90*, 473–482.

Gerard, V. A. (1988). Ecotypic differentiation in light-related traits of the kelp *Laminaria saccharina*. *Marine Biology*, *97*, 25–36.

Gerard, V. A., & Du Bois, K. R. (1988). Temperature ecotypes near the southern boundary of the kelp *Laminaria saccharina*. *Marine Biology*, *97*, 575–580.

Gévaert, F., Créach, A., Davoult, D., Migné, A., Levavasseur, G., Arzel, P., Holl, A. C., & Lemoine, Y. (2003). *Laminaria saccharina* photosynthesis measured in situ: Photoinhibition and xanthophyll cycle during a tidal cycle. *Marine Ecology Progress Series*, *247*, 43–50.

Gévaert, F., Delebecq, G., Menu, D., & Brutier, L. (2011). A fully automated system for measurements of photosynthetic oxygen exchange under immersed conditions: An example of its use in *Laminaria digitata* (Heterokontophyta: Phaeophyceae). *Limnology and Oceanography: Methods*, *9*, 361–379.

Gómez, I., Español, S., Véliz, K., & Huovinen, P. (2016). Spatial distribution of phlorotannins and its relationship with photosynthetic UV tolerance and allocation of storage carbohydrates in blades of the kelp *Lessonia spicata*. *Marine Biology*, *163*, 1–14.

Gómez, I., Orostegui, M., & Huovinen, P. (2007). Morpho-functional patterns of photosynthesis in the South Pacific kelp *Lessonia nigrescens*: Effects of UV radiation on ^{14}C fixation and primary photochemical reactions. *Journal of Phycology*, *43*, 55–64.

Gómez, I., Weykam, G., Klöser, H., & Wiencke, C. (1997). Photosynthetic light requirements, metabolic carbon balance and zonation of sublittoral macroalgae from King George Island (Antarctica). *Marine Ecology Progress Series*, *148*, 281–293.

Granbom, M., Pedersén, M., Kadel, P., & Lüning, K. (2001). Circadian rhythm of photosynthetic oxygen evolution in *Kappaphycus alvarezii* (Rhodophyta): Dependence on light quantity and quality. *Journal of Phycology*, *37*, 1020–1025.

Grevby, C., Axelsson, L., & Sundqvist, C. (1989). Light-independent plastid differentiation in the brown alga *Laminaria saccharina* (Phaeophyceae). *Phycologia*, *28*, 375–384.

Hanelt, D. (1998). Capability of dynamic photoinhibition in Arctic macroalgae is related to their depth distribution. *Marine Biology*, *131*, 361–369.

Hanelt, D. (2018). Photosynthesis assessed by chlorophyll fluorescence. In D. P. Häder & G. S. Erzinger (Eds.), *Bioassays, advanced methods and applications* (pp. 169–198). Elsevier.

Hanelt, D., Huppertz, K., & Nultsch, W. (1993). Daily course of photosynthesis and photoinhibition in marine macroalgae investigated in the laboratory and field. *Marine Ecology Progress Series*, *97*, 31–37.

Hanelt, D., Tüg, H., Bischof, K., Groß, C., Lippert, H., Sawall, T., & Wiencke, C. (2001). Light regime in an Arctic fjord: A study related to stratospheric ozone depletion as a basis for determination of UV effects on algal growth. *Marine Biology*, *138*, 649–658.

Hatcher, B. (1977). An apparatus for measuring photosynthesis and respiration of intact large marine algae and comparison of results with those from experiments with tissue segments. *Marine Biology*, *43*, 381–385.

Henley, W. J., Levavasseur, G., Franklin, L. A., Lindley, S. T., Ramus, J., & Osmond, C. B. (1991). Diurnal responses of photosynthesis and fluorescence in *Ulva rotundata* acclimated to sun and shade in outdoor culture. *Marine Ecology Progress Series*, *75*, 19–28.

Iñiguez, C., Carmona, R., Lorenzo, M. R., Niell, F. X., Wiencke, C., & Gordillo, F. J. L. (2016). Increased CO_2 modifies the carbon balance and the photosynthetic yield of two common Arctic brown seaweeds: *Desmarestia aculeata* and *Alaria esculenta*. *Polar Biology*, *39*, 1979–1991.

Inskeep, W. P., & Bloom, P. R. (1985). Extinction coefficients of chlorophyll a and b in N, N-dimethylformamide and 80% acetone. *Plant Physiology*, *77*, 483–485.

Jassby, A. D., & Platt, T. (1976). Mathematical formulation of the relationship between photosynthesis and light for phytoplankton. *Limnology and Oceanography*, *21*, 540–547.

Johansson, G., & Snoeijs, P. (2002). Macroalgal photosynthetic responses to light in relation to thallus morphology and depth zonation. *Marine Ecology Progress Series*, *244*, 63–72.

Johnston, A. M., & Raven, J. A. (1986). The utilization of bicarbonate ions by the macroalga *Ascophyllum nodosum* (L.) Le Jolis. *Plant, Cell & Environment*, *9*, 175–184.

Kain, J. M. (1979). A view of the genus *Laminaria*. *Oceanography and Marine Biology: An Annual Review*, *17*, 101–161.

Kain, J. M., & Jones, N. S. (1976). The biology of *Laminaria hyperborea* IX. Growth pattern of fronds. *Journal of the Marine Biological Association of the United Kingdom*, *56*, 603–628.

Kain, J. M., & Jones, N. S. (1977). The biology of *Laminaria hyperborea* X. the effect of depth on some populations. *Journal of the Marine Biological Association of the United Kingdom*, *57*, 587–607.

King, R. J., & Schramm, W. (1976). Determination of photosynthetic rates for the marine algae *Fucus vesiculosus* and *Laminaria digitata*. *Marine Biology*, *37*, 209–213.

Kirk, J. T. (1994). *Light and photosynthesis in aquatic ecosystems*. Cambridge University Press.

Koch, K., Thiel, M., Hagen, W., Graeve, M., Gómez, I., Jofre, D., Hofmann, L. C., Tala, F., & Bischof, K. (2016). Short-and long-term acclimation patterns of the giant kelp *Macrocystis pyrifera* (Laminariales, Phaeophyceae) along a depth gradient. *Journal of Phycology*, *52*, 260–273.

Krause-Jensen, D., Archambault, P., Assis, J., Bartsch, I., Bischof, K., Filbee-Dexter, K., Dunton, K. H., Maximova, O., Ragnarsdóttir, S. B., Sejr, M. K., Simakova, U., Spiridonov, V., Wegeberg, S., Winding, M. H. S., & Duarte, C. M. (2020). Imprint of climate change on pan-Arctic marine vegetation. *Frontiers in Marine Science*, *7*, 1129.

Krause-Jensen, D., & Duarte, C. M. (2016). Substantial role of macroalgae in marine carbon sequestration. *Nature Geoscience*, *9*, 737–742.

Krause-Jensen, D., Marbà, N., Olesen, B., Sejr, M. K., Christensen, P. B., Rodrigues, J., Renaud, P. E., Balsby, T. J. S., & Rysgaard, S. (2012). Seasonal Sea ice cover as principal driver of spatial and temporal variation in depth extension and annual production of kelp in Greenland. *Global Change Biology*, *18*, 2981–2994.

Krüger, M. (2016). *Photosynthese-Lichtkurven ausgewählter Makroalgenarten des Kongsfjords (Spitzbergen, Norwegen) als Grundlage für Abschätzungen zur Produktivität des arktischen Kelpwaldes*.[Diploma thesis,. Technical University of Freiberg].

Krumhansl, K. A., & Scheibling, R. E. (2012). Production and fate of kelp detritus. *Marine Ecology Progress Series*, *467*, 281–302.

Küppers, U., & Kremer, B. P. (1978). Longitudinal profiles of carbon dioxide fixation capacities in marine macroalgae. *Plant Physiology*, *62*, 49–53.

Kylin, H. (1947). Die Phaeophyceen der schwedischen Westküste. *Lunds Univ. Årsskr. (Avd. 2)*, *43*, 1–99.

Lee, Z., Shang, S., Du, K., & Wie, J. (2018). Resolving the longstanding puzzles about the observed Secchi depth relationships. *Limnology and Oceanography*, *63*, 2321–2336.

Littler, M. M., & Littler, D. S. (1980). The evolution of thallus form and survival strategies in benthic marine macroalgae: Field and laboratory tests of a functional form model. *The American Naturalist*, *116*, 25–44.

Liu, Z., Wang, Q., Zou, D., & Yang, Y. (2018). Effects of selenite on growth, photosynthesis and antioxidant system in seaweeds, *Ulva fasciata* (Chlorophyta) and *Gracilaria lemaneiformis* (Rhodophyta). *Algal Research*, *36*, 115–124.

Lüder, U. H., & Clayton, M. N. (2004). Induction of phlorotannins in the brown macroalga *Ecklonia radiata* (Laminariales, Phaeophyta) in response to simulated herbivory—The first microscopic study. *Planta*, *218*, 928–937.

Lüning, K. (1969). Standing crop and leaf area index of the sublittoral *Laminaria* species near Helgoland. *Marine Biology*, *3*, 282–286.

Lüning, K. (1979). Growth strategies of three *Laminaria* species (Phaeophyceae) inhabiting different depth zones in the sublittoral region of Helgoland (North Sea). *Marine Ecology Progress Series*, *1*, 195–207.

Lüning, K. (1981). Light. In C. S. Lobban & M. J. Wynne (Eds.), *The biology of seaweeds* (pp. 326–355). Blackwell Scientific Publishers.

Lüning, K. (1990). *Seaweeds: Their environment, biogeography, and ecophysiology*. John Wiley & Sons.

Lüning, K., & Dring, M. J. (1979). Continuous underwater light measurement near Helgoland (North Sea) and its significance for characteristic light limits in the sublittoral region. *Helgoländer Wissenschaftliche Meeresuntersuchungen*, *32*, 403–424.

Mabin, C. J., Johnson, C. R., & Wright, J. T. (2019). Physiological response to temperature, light, and nitrates in the giant kelp *Macrocystis pyrifera* from Tasmania, Australia. *Marine Ecology Progress Series*, *614*, 1–19.

Machalek, K. M., Davison, I. R., & Falkowski, P. G. (1996). Thermal acclimation and photoacclimation of photosynthesis in the brown alga *Laminaria saccharina*. *Plant Cell & Environment*, *19*, 1005–1016.

Mann, K. H. (2000). *Ecology of coastal waters. With implications for management*. Blackwell Science Publishers.

Marambio, J., Rodriguez, J. P., Mendex, F., Ocaranza, P., Rosenfeld, S., Ojeda, J., Rautenberger, R., Bischof, K., Terrados, J., & Mansilla, A. (2017). Photosynthetic performance and pigment composition of *Macrocystis pyrifera* (Laminariales, Phaeophyceae) along a gradient of depth and seasonality in the ecoregion of Magellan, Chile. *Journal of Applied Phycology*, *29*, 2575–2585.

Matthes, L. C., Ehn, J. K., Dalman, L. A., Babb, D. G., Peeken, I., Harasyn, M., Kirillov, S., Lee, J., Bélanger, S., Tremblay, J. É., Barber, D. G., & Mundy, C. J. (2021). Environmental drivers of spring primary production in Hudson Bay. *Elementa: Science of the Anthropocene*, *9*, 160.

Miller, H. L., III, Neale, P. J., & Dunton, K. H. (2009). Biological weighting functions for UV inhibition of photosynthesis in kelp *Laminaria hyperborea* (Phaeophyceae). *Journal of Phycology*, *45*, 571–584.

Morris, D. P., Zagarese, H., Williamson, C. E., Balseiro, E. G., Hargreaves, B. R., Modenutti, B., Moeller, R., & Queimalinos, C. (1995). The attenuation of solar UV radiation in lakes and the role of dissolved organic carbon. *Limnology and Oceanography*, *40*, 1381–1391.

Pedersen, M. F., Filbee-Dexter, K., Norderhaug, K. M., Fredriksen, S., Frisk, N. L., & Wernberg, T. (2020). Detrital carbon production and export in high latitude kelp forests. *Oecologia*, *192*, 227–239.

Pedersen, M. F., Nejrup, L. B., Fredriksen, S., Christie, H., & Norderhaug, K. M. (2012). Effects of wave exposure on population structure, demography, biomass and productivity of the kelp *Laminaria hyperborea*. *Marine Ecology Progress Series*, *451*, 45–60.

Pedersen, M. F., Nejrup, L. B., Pedersen, T. M., & Fredriksen, S. (2014). Sub-canopy light conditions only allow low annual net productivity of epiphytic algae on kelp *Laminaria hyperborea*. *Marine Ecology Progress Series*, *516*, 163–176.

Pehlke, C., & Bartsch, I. (2008). Changes in depth distribution and biomass of sublittoral seaweeds at Helgoland (North Sea) between 1970 and 2005. *Climate Research*, *37*, 135–147.

Rodgers, K. L., & Shears, N. T. (2016). Modelling kelp forest primary production using in situ photosynthesis, biomass and light measurements. *Marine Ecology Progress Series*, *553*, 67–79.

Schreiber, U., Schliwa, U., & Bilger, W. (1986). Continuous recording of photochemical and non-photochemical chlorophyll fluorescence quenching with a new type of modulation fluorometer. *Photosynthesis Research*, *10*, 51–62.

Schubert, H., Gerbersdorf, S., Titlyanov, E., Titlyanova, T., Granbom, M., Pape, C., & Lüning, K. (2004). Circadian rhythm of photosynthesis in *Kappaphycus alvarezii* (Rhodophyta): Independence of the cell cycle and possible photosynthetic clock targets. *European Journal of Phycology*, *39*, 423–430.

Smale, D. A., Pessarrodona, A., King, N., Burrows, M. T., Yunnie, A., Vance, T., & Moore, P. (2020). Environmental factors influencing primary productivity of the forest-forming kelp *Laminaria*

hyperborea in the Northeast Atlantic. *Scientific Reports*, *10*, 1–12.

Staehr, P. A., & Wernberg, T. (2009). Physiological responses of *Ecklonia radiata* (Laminariales) to a latitudinal gradient in ocean temperature. *Journal of Phycology*, *45*, 91–99.

Steinberg, R. (2019). *Investigation of the Helgoland kelp forest along a depth gradient.*[Master's thesis, Carl von Ossietzky University of Oldenburg].

Steinbiss, H. H., & Schmitz, K. (1974). Zur Entwicklung und funktionellen Anatomie des Blades von *Laminaria hyperborea*. *Helgoländer Wissenschaftliche Meeresuntersuchungen*, *26*, 134–152.

Steneck, R. S., Graham, M. H., Bourque, B. J., Corbett, D., Erlandson, J. M., Estes, J. A., & Tegner, M. J. (2002). Kelp forest ecosystems: Biodiversity, stability, resilience and future. *Environmental Conservation*, *29*, 436–459.

Tengberg, A., Hovdenes, J., Andersson, H. J., Brocandel, O., Diaz, R., Hebert, D., Arnerich, T., Huber, C., Körtzinger, A., Khripounoff, A., Rey, F., Rönning, C., Schimanski, J., Somme, S., & Stangelmayer, A. (2006). Evaluation of a lifetime-based optode to measure oxygen in aquatic systems. *Limnology and Oceanography: Methods*, *4*, 7–17.

tom Dieck, I. (1992). North Pacific and North Atlantic digitate *Laminaria* species (Phaeophyta): Hybridization experiments and temperature responses. *Phycologia*, *31*, 147–163.

Uhl, F., Bartsch, I., & Oppelt, N. (2016). Submerged kelp detection with hyperspectral data. *Remote Sensing*, *8*, 487.

White, L., Loisel, S., Sevin, L., & Davoult, D. (2021). In situ estimates of kelp forest productivity in macro-tidal environments. *Limnology and Oceanography*, *66*, 4227–4239.

SUPPORTING INFORMATION

Additional supporting information can be found online in the Supporting Information section at the end of this article.

Figure S1. Experimental scheme from sampling and cutting the blade discs for the two experiments (blade gradient and depth gradient) until the final oxygen measurements with subsequent chlorophyll analysis.

Table S1. Photon flux densities (PFD) of the three used slide projectors during the incubation experiments.

Table S2. Mean daily net primary production rates (NPPs) along the depth gradient of 0.5, 2, 4, and 6 m for different diffuse vertical attenuation coefficients (K_d).

Table S3. Post hoc test for Kruskal–Wallis ANOVAs. Net primary production rates (NPP) along the depth gradient were modulated based on daily diffuse vertical attenuation coefficients (K_d). NPP modulated with daily K_d (Table S3) were compared to NPP either modulated with mean K_d (Mean, $0.46\,m^{-1}$), lowest calculated K_d (Min, $0.28\,m^{-1}$), and highest calculated K_d (Max, $0.87\,m^{-1}$; each depth $n = 50$). Significance level: $p < 0.05$.

Table S4. Dry mass (DM): area ratios of *Laminaria hyperborea* blade discs from different depth and along the blade gradient.